UNIVERSITÉ DE MONTRÉAL

HEAT TRANSFER IN OPEN CAVITIES FROM DISCRETE HEATERS AT THEIR OPTIMUM POSITIONS

ALTAN MUFTUOGLU
DÉPARTEMENT DE GÉNIE MÉCANIQUE
ÉCOLE POLYTECHNIQUE DE MONTRÉAL

MÉMOIRE PRÉSENTÉ EN VUE DE L'OBTENTION
DU DIPLÔME DE MAÎTRISE ÈS SCIENCES APPLIQUÉES
(GÉNIE MÉCANIQUE)
AVRIL 2007

Your file Votre référence
ISBN: 978-0-494-29244-0
Our file Notre référence
ISBN: 978-0-494-29244-0

UNIVERSITÉ DE MONTRÉAL
ÉCOLE POLYTECHNIQUE DE MONTRÉAL

Ce mémoire intitulé :

HEAT TRANSFER IN OPEN CAVITIES FROM DISCRETE HEATERS AT THEIR OPTIMUM POSITIONS

présenté par : MUFTUOGLU Altan
en vue de l'obtention du diplôme de : Maîtrise ès sciences appliquées
a été dûment accepté par le jury d'examen constitué de :

M. NGUYEN T. Hung, Ph.D., président
M. BILGEN Ertugrul, Ph.D., membre et directeur de recherche
M. REGGIO Marcelo, Ph.D., membre

DÉDICACE

À mes parents

ACKNOWLEDGMENT

I would like to thank Professor Ertugrul BILGEN, my supervisor, for his support. His motivation and assistance have been substantial. I appreciate the efforts of my committee members, Professors T. Hung NGUYEN and Marcelo REGGIO. I would also like to thank my friends and members of Mechanical Engineering Department at Ecole Polytechnique de Montreal who were always there to answer my questions, listening me to talk to them and teach me French.

Special thanks to my friend, Tibet, for her patience, encouragement and suggestions. Also, I should express my appreciation to my entire family, especially my mom, dad and sister who always loved and supported me until now.

ABSTRACT

In this study, we determined optimum positions of discrete heaters by maximizing the conductance and then studied heat transfer and volume flow rate with discrete heaters at their optimum positions. Two different cases were investigated: i) small number of discrete heaters with finite size placed on adiabatic vertical wall in an open square cavity, and ii) a heater placed at its optimum position on the wall with finite thickness and conductance in open cavities with various aspect ratios. Continuity, Navier-Stokes and energy equations are solved by finite control volume numerical method.

The relevant governing parameters for the first case were: the Rayleigh numbers, Ra from 10^3 to10^7, the cavity aspect ratio, $A=H/L=1$, the heater size h/L from 0.05 to 0.20 and number of heaters from 1 to 3. For the second case, the relevant governing parameters were: the Rayleigh numbers, Ra from 10^6 to 10^{12}, the Prandtl number, $Pr=0.7$, the cavity aspect ratio, $A=H/L$ from 0.5 to 2, the wall thickness ℓ/L from 0.05 to 0.15, the heater size h/L from 0.15 to 0.6.

We found for the first case that the global conductance is as an increasing function of the Rayleigh number, the heater size and the number of heaters. Best thermal performance is obtained by positioning the discrete heaters closer to the bottom and closer to each other at the beginning of fluid flow. The configuration is not equidistance but follows a function of the Rayleigh number. The Nusselt number and the volume flow rate in and

out the open cavity are also increasing functions of the Rayleigh number, the heater size and the number of heaters.

Second case revealed that the global conductance is an increasing function of the Rayleigh number, the conductivity ratio, and a decreasing function of the wall thickness. Best thermal performance is obtained by positioning the discrete heater at off center and slightly closer to the bottom. The Nusselt number and the volume flow rate in and out the open cavity are an increasing function of the Rayleigh number and the wall thickness, and a decreasing function of the conductivity ratio. The Rayleigh number is a decreasing function of the cavity aspect ratio and the volume flow rate is an increasing function of it.

RÉSUMÉ

Dans cette étude, l'objectif est de déterminer la position optimale de chauffeurs discrètement placés sur une paroi en maximisant la conductance et ensuite en étudiant le transfert de chaleur et le débit volumique du fluide avec les chauffeurs à leur position optimale.

Deux cas ont été principalement étudiés : i) un certain nombre de chauffeurs discrets avec des dimensions finis est placé sur une plaque verticale adiabatique dans une cavité ouverte; ii) un chauffeur placé à la position optimale déterminée sur un mur d'épaisseur et de conductance finies dans des cavités ouvertes de différent rapport de forme. Les équations de continuité, de Navier – Stokes et de l'énergie sont résolues avec la méthode des volumes de contrôle.

Les paramètres déterminants dans le premier cas sont: le nombre de Rayleigh, Ra (de 10^3 à 10^7), le rapport de forme, $A=H/L=1$, la dimension du chauffeur, h/L (de 0.05 à 0.20), le nombre total de chauffeur (de 1 à 3). Pour le second cas, les paramètres déterminants sont : le nombre de Rayleigh, Ra (de 10^6 à 10^{12}), le nombre de Prandtl, $Pr=0.7$ (pour l'air), le rapport de forme $A=H/L$ (de 0.5 à 2), l'épaisseur du mur ℓ/L (de 0.05 à 0.15), la dimension du chauffeur h/L (de 0.15 à 0.60).

Les résultats pour le premier cas montrent que la conductance augmente en fonction du nombre de Rayleigh, *Ra*, de la dimension du chauffeur, *h/L,* et du nombre de chauffeur, *N*. La meilleure performance est obtenue en plaçant les chauffeurs proche de la base de la cavité et plus près les uns des autres à l'entrée de l'écoulement du fluide. La configuration n'est pas équidistance; elle suit une fonction de Rayleigh. Le nombre de Nusselt, *Nu* et le débit volumique à l'entrée et la sortie de la cavité sont aussi croissants en fonction du nombre de Rayleigh, *Ra*, de la dimension du chauffeur, *h/L* et du nombre du chauffeur, *N*.

Le second cas montre que la conductance globale est une fonction croissante du nombre de Rayleigh, du rapport de conductivité, et une fonction décroissante de l'épaisseur du mur. La meilleure performance thermale est obtenue en plaçant le chauffeur pas exactement au centre plutôt légèrement proche de la base. Le nombre de Nusselt, *Nu* et le débit volumique à l'entrée et la sortie de la cavité sont des fonctions croissantes du nombre de Rayleigh, *Ra*, et de l'épaisseur du mur, ℓ/L, et des fonctions décroissantes du rapport de conductivité, k_r. Le nombre de Nusselt est une fonction décroissante du rapport de forme; par contre, le débit volumique est une fonction croissante.

CONDENSÉ

Notre objectif dans ce mémoire est d'étudier la performance thermique de chauffeurs discrets et leurs positions optimales dans des cavités ouvertes. La performance thermique des éléments électroniques contenant plusieurs sources de chaleur discrètes a été considérablement étudiée dans la littérature. Le problème de design dans les pièces électroniques est de maintenir un refroidissement efficace des puces de manière à empêcher la surchauffe et les points chauds. Ceci est généralement atteint par un refroidissement efficace par convection naturelle, convection mixte et dans certains cas, par des autres moyens, tels que l'utilisation de caloduc ou finalement un meilleur design. Dans ce dernier cas, l'objectif est de maximiser le transfert de chaleur pour que la température maximale spécifiée pour la sécurité de l'utilisation de la puce ne soit pas dépassée. Ainsi, le placement optimal des chauffeurs discrets par rapport à un placement équidistant généralement utilisé, pourrait être envisagé. Dans ce cadre, peu d'études théoriques et expérimentales ont été publiées.

Un examen de la littérature nous a montré que les pièces contenant des circuits intégrés chauffes discrètement ont été étudiées pour obtenir un mécanisme de refroidissement par la convection naturelle laminaire. Les paramètres principaux sont : la position de la plus grande protubérance, existante entre les composants électroniques et la distribution de la puissance dissipée. Les propriétés du fluide ont été prises constantes et les variations de

la densité du fluide ont été négligées sauf dans le terme de flottabilité. Les champs de flux et de température et le transfert de chaleur ont été examinés. Les résultats ont montré que la température maximum est sensible à la position de plus grands composants. Dans une autre étude, pour trouver la position optimale de trois sources de chaleur dans les cavités ouvertes en deux dimensions, 14 configurations différentes ont été aussi considérées dans lesquelles le nombre de Rayleigh a été varié de 10^4 à 10^5. Bien que les domaines aient été maillés séparément, le problème a été résolu en tenant compte des régions entières. Il a été montré qu'une position symétrique de la puce n'était pas la meilleure configuration en termes de transfert de chaleur. La meilleure performance thermique, ce qui signifie prévenir les points chauds et minimiser la température moyenne, a été atteinte quand les puces sont disposées avec une proportion géométrique de 1,618. D'après nous, cette étude pourrait être développée en augmentant le nombre de configurations géométriques et la gamme de nombre de Rayleigh de 10^3 à 10^8.

Une revue de littérature nous a montré que bien qu'il existe quelques études de transfert de chaleur avec des chauffeurs discrets à leurs positions optimisées, le cas des cavités ouvertes avec les chauffeurs discrets dans leurs positions optimales n'a pas été trouvé dans la littérature. Dans l'étude présente, nous examinerons deux cas différents : i) Un petit nombre de chauffeurs discrets avec dimensions finies sont placé sur mur adiabatique vertical dans une cavité carrée ouverte, ii) un chauffeur est placé à sa position optimale sur un mur avec épaisseur et conductance finie dans des cavités

ouvertes avec différent rapport de forme. Notre but est de déterminer les positions optimales des chauffeurs et étudier leur performance thermique quand ils sont placés à leurs positions optimales dans les cavités ouvertes.

Cette thèse est présentée en 5 chapitres, comprenant le Chapitre 1 en l'introduction. La définition de problème, le modèle mathématique et les équations régissantes, la conservation de la masse, la quantité de mouvement et de l'énergie avec les conditions aux frontières, de même que la méthode numérique, la vérification de code, et l'étude d'indépendance du maillage sont présentées dans le Chapitre 2. En ce qui concerne le Chapitre 3, il contient les résultats obtenus et la discussion pour le cas de la cavité carrée avec un nombre fini de chauffeurs discrets dans leurs positions optimum. Dans le Chapitre 4, nous présentons les résultats pour le cas des cavités avec le mur conducteur et un seul chauffeur discret à sa position optimale. Finalement, les conclusions générales sont présentées dans le Chapitre 5.

Les Cavités ouvertes sans le Mur Massif et avec un Nombre Fini de Chauffeurs Discrets:

Le problème est de déterminer la position optimale d'un, deux ou de plusieurs d'éléments chauffants discrets placés dans une cavité carrée ouverte, refroidie par la convection naturelle. Ensuite, la performance du transfert de chaleur de chaque cas est étudiée pour les positions optimales déterminées.

Une cavité carrée, ouverte et à deux dimensions avec trois éléments chauffants discrets est considérée avec les conditions aux frontières appropriées. Toutes les trois frontières solides de la cavité sont adiabatiques et le côté qui fait face à la frontière gauche verticale est ouvert à l'air ambiant. Un, deux ou trois éléments discrets chauffant sont installés sur la frontière gauche verticale. Chaque élément chauffant de hauteur h et coordonnées $(0, y_i)$ disperse un flux de chaleur constant, $q"$. L'air de refroidissement entre dans la cavité d'un réservoir par la partie plus basse de l'ouverture ; il circule le long des éléments de chauffage et sort par la partie supérieure de l'ouverture.

Les Cavités Ouvertes avec le Mur Massif et un Chauffeur Discret Unique :

Tout d'abord, nous avons déterminé la position optimale d'un élément chauffant discret dans des cavités ouvertes installées sur un mur conductif faisant face à l'ouverture et refroidie par la convection naturelle. Ensuite, nous avons étudié la performance du transfert de chaleur pour plusieurs cas avec le chauffeur placé à sa position optimale. Enfin, une étude de sensibilité sur les paramètres gouvernants est menée.

Les frontières horizontales de la cavité sont adiabatiques, la face gauche du mur solide est isotherme et l'autre côté du mur est en contact avec l'air d'ambiant. Un élément chauffant discret est installé sur le mur solide dans la cavité. Cet élément de hauteur h et coordonnées $(0, y_i)$ disperse un flux de chaleur constant, $q"$. L'air de refroidissement

entre dans la cavité d'un réservoir par la partie plus basse de l'ouverture ; il circule le long de l'élément de chauffage et sort par la partie supérieure de l'ouverture.

Nous supposons que le fluide est newtonien, les échanges radiatifs sont négligeables et la troisième dimension a un effet négligeable sur le transfert de chaleur. Avec ces hypothèses, nous avons utilisé les équations de conservation en deux dimensions pour la masse, quantité de mouvement avec l'approximation de Bussinesq et l'énergie. En utilisant L comme longueur caractéristique, α/L comme vitesse caractéristique, $Lq"/k$ comme température caractéristique et L^2/α pour l'échelle de temps, nous avons obtenu des équations adimensionnelles de masse, quantité de mouvement et l'énergie.

Les paramètres gouvernants sont $Ra = g\beta q" L^4/(\upsilon\alpha k)$, $Pr = \upsilon/\alpha$, et A, h/L, et dans le cas de la cavité ouverte avec un mur massif ils sont Ra, Pr, A, k_r et le ℓ/L.

La méthode numérique utilisée pour résoudre le système d'équations avec les conditions aux frontières pour le cas du mur non massif et pour le cas du mur massif est la méthode SIMPLER. Un code informatique, basé sur la formulation mathématique présentée ci-dessus et la méthode SIMPLER a été validée par rapport à des études dans la littérature. Les résultats de cette validation ont montré un excellent accord. De plus, la comparaison du nombre de Nusselt moyen sur les murs chauds et froids a montré une différence maximum d'environ 0,5% dans toutes les simulations. Le code présent a aussi été utilisé pour simuler le cas des cavités ouvertes avec un domaine de calcul agrandi. Pour cette

étude, nous avons utilisé un domaine de calcul limité à la cavité et avons comparé les résultats avec ceux du domaine de calcul agrandi. Les résultats ont montré un bon accord.

Un maillage uniforme dans les directions X et Y a été utilisé pour tous calculs. La convergence du maillage a été étudiée pour le cas $A = 1$ avec les tailles de maillage de 21x21 à 151x151 à $Ra = 10^5$ et 10^7. Pour 81x81 et 101x101, les variations de Nu etla conductance C sont respectivement $6.2\text{x}10^{-4}$ et $1.27\text{x}10^{-2}$, à $Ra=10^5$, et ils sont respectivement de $2.1\text{x}10^{-3}$ et $1.3\text{x}10^{-2}$, à $Ra=10^7$. Alors, nous avons fait un compromis entre le temps de calcul et la précision, et nous avons choisi une taille de maillage de 81x81. Avec l'utilisation d'un système avec un microprocesseur de 3,2 GHz, pour un maillage de 81x81, à $Ra=10^6$, le temps d'exécution typique est 92 s pour le cas d'un chauffeur unique et 76 s pour le cas de 3 chauffeurs.

Une solution est obtenue en effectuant des itérations dans le temps jusqu'à ce que les variations dans les variables primitives entre les étapes de temps subséquentes soient inférieures à 10^{-4}.

Dans un pas de temps, le résiduel du terme de pression doit être inférieure à 10^{-3}. De plus, la précision de la solution est revérifié en utilisant la conservation d'énergie sur le domaine pour s'assurer la perte d'énergie soit inférieure à 10^{-4}.

Dans le cas de la convection naturelle dans une cavité carrée ouverte avec les chauffeurs discrets, les paramètres gouvernants sont : le rapport de forme A = 1, les paramètres variables considérés sont les dimensions de l'élément chauffant h/L = 0.05, 0.10 et 0.20, le nombre d'éléments chauffant, N = 1, 2 et 3, et nombre de Rayleigh, $Ra = 10^3$ à 10^7, le nombre de Prandtl, Pr = 0.70 (pour l'air).

Dans le cas du transfert de chaleur conjugué dans des cavités ouvertes avec un chauffeur discret, les paramètres gouvernants sont : les paramètres géométriques variables comme le rapport de forme, A = 0,5, 1 et 2, et l'épaisseur de mur adimensionnelle, ℓ/L = 0.05, 0.10 et 0,15. La hauteur adimensionnelle d'élément chauffant, h/L = 0.15, 0.3 et 0,6 correspondant à A = 0.5, 1 et 2 respectivement. Ce qui résulte en un rapport constant entre les hauteurs du chauffeur et de la cavité. Le nombre de Rayleigh a été varié de 10^6 à 10^{12}. Le nombre de Prandtl, Pr = 0.70 pour l'air est supposé constant. Le rapport de conductivité a été varié de k_r =1 à 50.

L'objectif de déterminer la position optimale des éléments chauffants est atteint en conservant le nombre de chauffeur et leur dimension constant et en variant leur position. La procédure est la suivante : (i) on calcule la conductance $C(Y)$ pour une valeur de N et h/L donnés, à un Ra constant, (ii) on détermine la conduction maximum, C_{max} à la position optimale Y_{opt}. (iii) on répète les étapes (i) et (ii) pour déterminer $C(Y)$, C_{max} et Y_{opt} pour tous les autres nombres de Rayleigh, de 10^3 à 10^7, en conservant N et h/L constant. (iv) on répète les étapes (i) et (iii) pour obtenir la conductance maximum à la

position optimale, $C_{max}(Y_{opt})$ pour le même nombre de chauffeur, N, mais de tailles différentes h/L. Ensuite, on répète les étapes (ii) – (iv) pour obtenir la conductance maximum à la position optimale, $C_{max}(Y_{opt})$ pour le même nombre de chauffeur, N.

Les résultats obtenus sont présentés dans les figures :

Dans le premier cas, les lignes de courant et les isothermes sont tracées pour les nombres de Rayleigh différents. Le débit volumique et le nombre de Nusselt sont présentés en fonction du nombre de Rayleigh, de la taille et du nombre de chauffeur. Nous avons présenté une figure montrant l'évolution de la conductance en fonction de la position du chauffeur avec la taille du chauffeur comme paramètre et une autre avec un nombre de Rayleigh fixe et la taille du chauffeur comme paramètre. Nous avons trouvé que la conductance varie avec la position du chauffeur. Elle augmente graduellement quand la position du chauffeur va de la base vers une position proche de la mi-hauteur, et diminue par la suite jusqu'à la position la plus élevée. Le nombre de Nusselt et le débit volumique sont une fonction croissante du nombre de Rayleigh et la taille des chauffeurs.

Dans le deuxième cas, la conductance est tracée en fonction de la position du chauffeur avec la conductivité comme un paramètre. Les lignes de courant et les isothermes sont présentés dans les figures en fonction du nombre de Rayleigh et avec la conductivité comme paramètre. Le nombre Nusselt et le débit volumique sont présentés, en fonction

de l'épaisseur du mur et la conductivité en conservant le rapport de forme constant. Ces paramètres sont aussi présentés en fonction du rapport de forme, et de l'épaisseur du mur en gardant le rapport de la forme constant. On a trouvé que la conductance est une fonction croissante du nombre de Rayleigh et de la conductivité. De plus, nous avons trouvé que le débit volumique est une fonction décroissante de la conductivité. Nous avons constaté que le nombre du Nusselt est faiblement dépendant de l'épaisseur de mur pour $A = 1$, et fortement pour $A = 2$. Le nombre de Nusselt et le débit volumique augmentent en fonction de l'épaisseur du mur et du nombre de Rayleigh pour tous les cas avec un rapport de forme de 0,5 à 2.

Étant donné les résultats présentés, les points principaux peuvent être résumés comme suit :

- Pour une meilleure performance thermique de chauffeurs discrets installés sur un mur vertical en face de l'ouverture d'une cavité carrée, la position optimale n'est pas de la placer à l'équidistance entre eux. La position optimale est obtenue en maximisant la performance globale. Les chauffeurs sont disposés proches les uns des autres au début de l'écoulement du fluide. La configuration finale des chauffeurs discrets dépend du nombre de Rayleigh.

- La conductance globale maximum est quasi-indépendante de nombre de Rayleigh pour un chauffeur unique ou une paire de chauffeur avec h/L=0.05 pour

$Ra < 10^4$. La conductance globale maximum est fortement dépendante du nombre de Rayleigh dans les autres cas ; il augmente avec le nombre de Rayleigh. De même, la conductance globale maximum est augmentée avec le nombre et la dimension du chauffeur.

- Pour le cas de Rayleigh, $Ra < 10^4$, la conduction est dominante alors que pour les nombres de Rayleigh plus élevé, la convection devient le régime dominant. Généralement, le nombre de Nusselt et le débit volumique augmentent en fonction du nombre de Rayleigh, de la taille et du nombre de chauffeurs discrets.

- La position optimale d'un chauffeur discret dans une cavité ouverte est généralement à outre du centre. Sa position dépend du nombre de Rayleigh, du rapport de conductivité, du rapport de forme et l'épaisseur de mur.

- En fonction du rapport de forme de la cavité et du rapport de conductivité, le transfert de chaleur est dominé par la conduction pour des nombres de Rayleigh faibles, Ra de 10^6 à 10^8 ; la convection devient dominante pour des nombres de Rayleigh élevés allant jusqu'à 10^{12} dans cette étude. Généralement, le nombre de Nusselt et le débit volumique augmentent en fonction du nombre de Rayleigh et l'épaisseur de mur. Le nombre de Rayleigh est une fonction décroissante du rapport de forme de la cavité et du rapport de conductivité; le débit volumique est une fonction croissante du rapport de forme de la cavité et décroissante du

rapport de conductivité. Les paramètres *Ra, A,* k_r sont significatifs et le paramètre ℓ/L est relativement moins en ce qui concerne la performance thermique des chauffeurs à leur position optimale.

- Dans certain cas des études sans et avec le mur conductif, en déterminant la conductance maximum, nous avons observé des optimums étendus de C par rapport à Y. Dans la pratique, aucune difficulté n'a été trouvée pour déterminer la position optimum d'un chauffeur, puisque les résultats numériques ont montré clairement la conductance maximum et ses coordonnées. D'autre part, nous notons que ces optimums étendus peuvent donner une certaine flexibilité de design pour positionner les chauffeurs dans des circonstances nécessaires.

CONTENTS

DÉDICACE iv

ACKNOWLEDGMENT v

ABSTRACT vi

RÉSUMÉ viii

CONDENSÉ x

CONTENTS xxi

FIGURE LIST xxiii

TABLE LIST xxvii

NOMENCLATURE xxviii

CHAPTER 1 INTRODUCTION 1

1.1.Objectives 1

1.2.Literature Review 2

CHAPTER 2 PROBLEM AND MATHEMATICAL MODEL 9

2.1.Problems 9

2.1.1.Open Cavities without Massive Wall and with Finite Number of Discrete Heaters 9

2.1.2.Open Cavities with Massive Wall and with a Single Discrete Heater 10

2.2.Mathematical Model 10

2.2.1.Boundary Conditions 13

2.2.1.1.Open Cavities without Massive Wall 13

2.2.1.2.Open Cavities with Massive Wall 13

2.3.Numerical Technique 14

CHAPTER 3 NATURAL CONVECTION IN AN OPEN SQUARE CAVITY WITH DISCRETE HEATERS AT THEIR OPTIMIZED POSITIONS 18

3.1.Introduction 18

3.2.Optimization Study 18

3.3.Heat Transfer and Volume Flow Rate 29

3.4.Conclusion 36

CHAPTER 4 CONJUGATE HEAT TRANSFER IN OPEN CAVITIES WITH A DISCRETE HEATER AT ITS OPTIMIZED POSITION 38

4.1.Introduction 38

4.2.Optimization Study 39

4.3.Heat Transfer and Volume Flow Rate 44

4.4.Conclusion 54

CHAPTER 5 GENERAL CONCLUSION 59

5.1.Introduction 59

5.2 In Case of Open Cavity without a Massive Wall and Single or Multi Heaters 59

5.3.In Case of Open Cavity with a Massive Wall and Single-Heater 60

REFERENCES 62

FIGURE LIST

Figure 1.1: Schematic of the square cavity with discrete heaters, the coordinate system and boundary conditions.....7

Figure 1.2: Schematic of the cavity with a conductive wall, a discrete heater, the coordinate system and boundary conditions.....7

Figure 3.1: The maximization of the global conductance when only one heat source is present.....20

Figure 3.2: Streamlines (on the left) and isotherms (on the right) for h/L=0.10,the most lower heater position (the upper figure), the optimum heater position (the lower figure, (a) Ra=10^3, Y_{opt} (the upper and lower figure)= 0.0 and 0.41, (b) Ra=10^5, Y_{opt} (the upper and lower figure) = 0.0 and 0.39, (c) Ra=10^7, Y_{opt} (the upper and lower figure) = 0.0 and 0.38.....22

Figure 3.3: (a) The optimal heater location and (b) corresponding maximum global conductance as a function of the Rayleigh number for the single heat source.....24

Figure 3.4: (a) The optimal heater location and (b) corresponding maximum global conductance as a function of the Rayleigh number for two heat sources.....26

Figure 3.5: (a) The optimal heater location and (b) corresponding maximum global conductance as a function of the Rayleigh number for three heat sources.....27

Figure 3.6: (a) Nusselt number and (b) flow rate as a function of the Rayleigh number for the single heat source of three sizes.....30

Figure 3.7: (a) Nusselt number and (b) flow rate as a function of the Rayleigh number for the two heat sources of three sizes.....32

Figure 3.8: (a) Nusselt number and (b) flow rate as a function of the Rayleigh number for the three heat sources of three sizes.....33

Figure 3.9: Streamlines (on the left) and isotherms (on the right) with h/L=0.10 and Ra=10^6. (a) One heater at its optimum position, Y_{opt}=0.38, (b) two heaters at their optimum positions, Y_{opt} = 0.09 and 0.49, (c) three heaters at their optimum positions, Y_{opt} = 0.06, 0.28 and 0.58.....35

Figure 4.1: The maximization of the global conductance with the heat source of h/L =0.30. The scales of the curves for k_r=1 and 50 are 4C and 0.25C = abscissa value respectively.....41

Figure 4.2: Streamlines (on the left) and isotherms (on the right) for A=1, ℓ/L =0.10, for a) Ra=10^6, b) Ra=10^8 and c) Ra=10^{10}. The upper figure is for k_r = 1 and the lower figure is for k_r = 10 for each case.....43

Figure 4.3: Maximum conductance as a function of the Rayleigh number with the conductivity ratio as a parameter. The scales of the curves for k_r=10 and 50 are (1/3)C_{max} and 0.1C_{max} = ordinate value respectively.....45

Figure 4.4: (a-c) Nusselt number and (d-f) volume flow rate as a function of Rayleigh number for A = 1 with ℓ/L and k_r as parameters. Solid line: ℓ/L =0.05, dotted line: ℓ/L =0.10, dashed line: ℓ/L =0.15.....47

Figure 4.5: (a-c) Nusselt number and (d-f) volume flow rate as a function of Rayleigh number for k_r =50, h/L=0.15 for A=0.5, h/L=0.30 for A=1 and h/L=0.60 for A=2 with ℓ/L and A as parameters. Solid line: ℓ/L =0.05, dotted line: ℓ/L =0.10, dashed line: ℓ/L =0.15.....49

Figure 4.6: (a) Nusselt number and (b) volume flow rate as a function of the aspect ratio at various Rayleigh numbers.....51

Figure 4.7: Streamlines (on the left) and isotherms (on the right) for the case of Fig. 4.6 (ℓ/L =0.10, k_r = 50) and Ra=10^8. a) A=0.5, h/L = 0.15, b) A=1, h/L = 0.30, and c) A=2, h/L = 0.60.....53

Figure 4.8: (a) Nusselt number and (b) flow rate as a function of the conductivity ratio with the Rayleigh number as a parameter.....55

Figure 4.9: (a) Nusselt number and (b) volume flow rate as a function of the wall thickness with the Rayleigh number as a parameter.....56

TABLE LIST

Table 2.1: Comparison of the benchmark results [15] at $x = 0$ and $x = ½$ plane.....15

Table 2.2: Comparison of the results with the enlarged domain [10] and the cavity restricted domain used in this study.....15

Table 2.3: Grid independence study results with $A = 1$ at $Ra = 10^5$ and 10^7.....17

Table 2.4: Grid independence study results with A=1, ΔL =0.10, k_r =10.....17

NOMENCLATURE

A	enclosure aspect ratio, $= H/L$
c_p	heat capacity, $J/kg \cdot K$
g	acceleration due to gravity, m/s^2
H	cavity height, m
h	heater size, m
k	thermal conductivity, $W/m \cdot K$
L	cavity width, m
ℓ	wall thickness, m
Nu	Nusselt Number, defined by equation 6
n	coordinate in any direction
P	dimensionless pressure, $= (p - p_\infty)L^2/\rho\alpha^2$
p	pressure, Pa
Pr	Prandtl number, $= \upsilon/\alpha$
$q"$	heat flux, W/m^2
q	dimensionless heat flux, $= \dfrac{\partial\theta}{\partial X}$
Ra	Rayleigh number, $= g\beta q" L^4/(\upsilon\alpha k)$
T	temperature, K
t	time, s

U, V dimensionless fluid velocities, $= uL/\alpha,\ vL/\alpha$

$\dot{V}$ dimensionless volume flow rate through the opening

X, Y dimensionless Cartesian coordinates, $= x/L,\ y/L,$

x, y Cartesian coordinates

Greek symbols

α thermal diffusivity, m^2/s

β volumetric coefficient of thermal expansion, $1/K$

υ kinematic viscosity, m^2/s

ρ fluid density, kg/m^3

ψ stream function

θ dimensionless temperature, $= (T - T_\infty)/(Lq''/k)$

τ dimensionless time, $= \alpha t/L^2$

Superscripts

- average

Subscripts

ext extremum

$_{in}$	into cavity
$_{max}$	maximum
$_{opt}$	optimum
$_{\infty}$	ambient value
$_{1, 2, 3}$	first, second and third heater

CHAPTER 1

INTRODUCTION

1.1. Objectives

Our objective in this memoir is to study thermal performance of discrete heaters in their optimum positions in open cavities. The thermal performance of electronic packages containing a number of discrete heat sources has been studied extensively in the literature. The design problem in electronic packages is to maintain cooling of chips in an effective way to prevent overheating and hot spots. This is achieved generally by effective cooling by natural convection, mixed convection and in certain cases, by other means, such as using heat pipes, and finally by better design. In the latter case, the objective is to maximize heat transfer density so that the maximum temperature specified for safe operation of a chip is not exceeded. Thus, optimum placement of discrete heaters with respect to usual equidistant placement may be required. In this respect, few theoretical and experimental studies have been published. In the following, we will review the literature on the subject of determination of optimum positions of discrete heaters in various geometries as well as on open cavities.

1.2. Literature Review

Wang et al. [1] studied discretely heated integrated circuit packages to observe cooling of board with discrete heaters by laminar natural convection. The multigrid technique was used to solve Navier-Stokes equations. The greatest protuberance location, spacing between electronic components and dissipated power distribution were the characteristic parameters. Properties of fluid were taken constant and density of fluid variations were neglected except in the buoyancy term. Flow and temperature fields and heat transfer were investigated. It was concluded that maximum temperature was sensitive to the position of bigger components. Liu and Phan-Tien [2] studied to find an optimum position of three heat sources in two dimensional open cavities. 14 different arrangements were considered and Rayleigh number was varied from 10^4 to 10^5. Although the regions were meshed separately, during the problem solving the whole case was taken into account. Finite element method was implemented numerically to solve the statement and satisfy Navier-Stokes equations. It was shown that symmetric chip positioning was not the best configuration in terms of heat transfer, and the best thermal performance, which means to prevent hot spots and minimize average temperature, was reached when the chips were positioned with a geometric ratio of 1.618. In our opinion, this study could be developed better by increasing the number of geometric arrangements and the range of Rayleigh number from 10^3 to 10^8, instead of from 10^4 to 10^5. Da Silva and his collaborators carried out several studies to determine optimum conditions for maximum performance in cooling applications in various

geometries [3-7]. Laminar natural convection was studied numerically to investigate the optimum position of discrete heaters with different number and size by Da Silva et al. [3]. Maximization of the global conductance between a horizontal wall and fluid and avoidance of hot spots when heat flux is fixed were the main purpose of the study. The optimum position of discrete heat sources was searched in an enclosed square cavity cooled by laminar natural convection, where the right wall had a constant temperature and the other three walls were adiabatic. Heat strips were situated on the left wall with constant heat flux. Firstly, one heat source was used and optimum position was obtained for different Rayleigh numbers. The same procedure was applied for two heat sources with different Rayleigh numbers. The results had revealed that as the Rayleigh number increased, the optimum position of the heat strips approached toward the bottom side of the wall. Also, it was found that the global conductance increased with the number of heat strips. The same trends were observed for the size of the heat strips, that is, the greater the size of the heat strips, the greater the global conductance. Optimum position of discrete heaters on a wall cooled in two dimensional channels by forced convection was also studied [4]. Large number of small heaters and small number of large heaters that were placed on a flat wall were analyzed in order to maximize the conductance between the wall and the fluid. The finite element code FIDAP was used to solve the mass, momentum and energy equations. Reynolds number range was 10^2-10^4. It was found that with increasing Reynolds number, heat strips got closer to the entrance of the channel and equidistance positioning of heaters was not an optimum solution in two dimensional open channels. They also showed that for a fixed heated area, the global

conductance increased with the number of optimally placed heaters. Da Silva et al. [5] conducted a numerical study to optimize the flow geometry of vertical diverging or converging channels to obtain maximum heat transfer rate density in laminar natural convection. The geometry was changed by varying the spacing between the walls, heat distribution along the walls and the angle between the two walls. The Rayleigh number was varied as $10^5 \leq Ra \leq 10^7$. It was found that using upper unheated sections increased the chimney effect and heat transfer. It was also found that the maximum heat transfer density was reached when the walls were parallel or nearly parallel. The optimal distribution and size of discrete heat sources in a vertical open channel cooled by natural convection, was investigated using the constructal method [6]. Heat sources with fixed size and fixed heat flux, and a single heat source with variable size and fixed total heat current were two considered cases. The aim of the study was maximization of the global thermal conductance between the cold fluid and discrete heaters. The Rayleigh number was varied from 10^2 to 10^4. They found that for the case of heat sources with fixed size and heat flux, the optimum location of heat sources changed with increasing Rayleigh numbers. The last heater's position shifted towards the exit plane, which in turn resulted in non-uniform distribution of heaters. For a variable size, single heat source at low and moderate Rayleigh numbers, the thermal performance was maximized when the heat source did not cover the entire wall. The geometric optimization of L and C-shaped channels in laminar natural convection subject to global constraints was studied by Da Silva and Gosselin [7]. With the objective of maximizing the heat transfer from the hot wall to the coolant fluid, three configurations were used: i) L-shaped asymmetric vertical

heated channel with an adiabatic horizontal inlet, ii) asymmetric vertical heated channel with an adiabatic vertical outlet, and iii) C-shaped vertical heated channel with horizontal inlet and outlet. The first two configurations were optimized in terms of wall-to-wall spacing and inlet (or outlet) height (two degrees of freedom), while the last one in terms of wall-to-wall spacing, inlet and outlet height (three degrees of freedom). A finite element commercial code was used to solve the conservation equations. The range of Rayleigh number was 10^5-10^7 and the Prandtl number was 0.7. The results showed the relevance of optimization with the number of degree of freedom. Numerical simulation results showed that optimum wall-to-wall spacing decreased as *Ra* increased and it was sensitive to the adiabatic extension length. The superiority of the performance of L-shaped channel configuration to the C-shaped channel was another conclusion.

A few studies on heat transfer in open cavities have been reported [8-13]. Numerical studies on open cavities have been studied aiming various applications. Open cavities with small aspect ratio, i.e. shallow cavities [8-10], inclined open square cavities [11], inclined shallow cavities with constant heat flux at the side facing the opening [12] and inclined shallow open cavities with a wall of finite thickness and with constant heat flux on the wall [13]. Among these, the most relevant studies to our case are those involving open cavities in which the wall facing the opening is heated by constant heat flux [12, 13]. A numerical study was done by Polat and Bilgen [12] on open cavities having the wall facing the opening heated at constant heat flux while two adjacent perpendicular walls were adiabatic. The cavity aspect ratio was from 1 to 0.125, i.e. shallow cavities,

the inclination was varied from vertical position to 45^{o} up facing position. The effects of aspect ratio, Rayleigh number and inclination angle on the heat transfer were reported. A subsequent study was carried out on conjugate heat transfer by conduction and natural convection in inclined open shallow cavities [13]. A conductive wall facing the opening was heated by constant heat flux while the other two perpendicular walls were adiabatic. The Simpler (Semi-implicit Method for Pressure Linked Equations Revised) algorithm was used to perform numerical analysis. Rayleigh number varied between 10^{6} and 10^{12} and the other governing parameters were wall to air conductivity ratio, cavity aspect ratio, dimensionless wall thickness, and inclination angle. It was shown that the volume flow rate increased with Rayleigh number, aspect ratio, dimensionless wall thickness and inclination angle and it decreased with conductivity ratio. Another conclusion was that the heat transfer increased with Rayleigh number and dimensionless wall thickness whereas it decreased with conductivity ratio.

We see from the above review that the case of open cavities with discrete heaters in their optimum positions has not been addressed in the literature. In the present study, we will investigate two different cases: i) small number of discrete heaters with finite size placed on adiabatic vertical wall in an open square cavity as given in Figure 1.1, ii) a heater placed at its optimum position on the wall with finite thickness and conductance in open cavities with various aspect ratios as given in Figure 1.2. Our aim is to determine optimum positions of the heaters and to study the thermal performance of optimally placed heaters in open cavities.

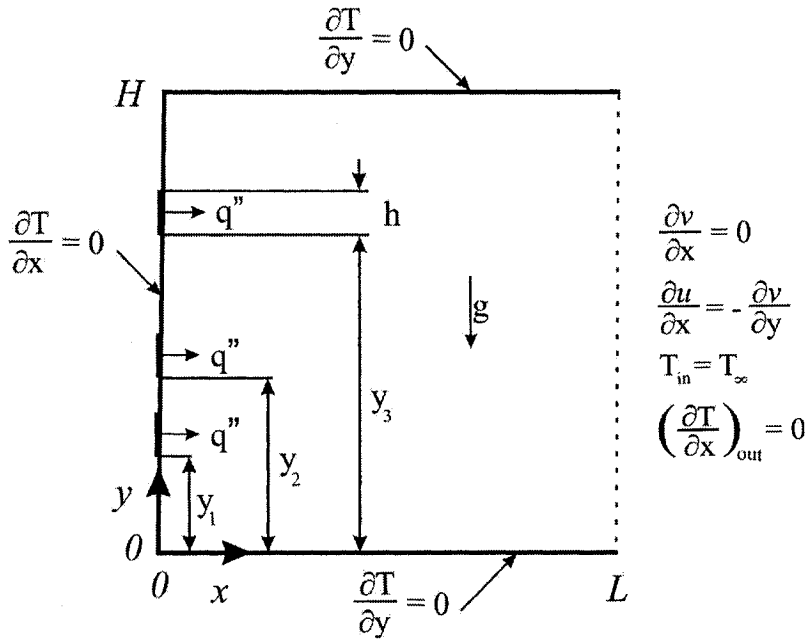

Figure 1.1: Schematic of the square cavity with discrete heaters, the coordinate system and boundary conditions.

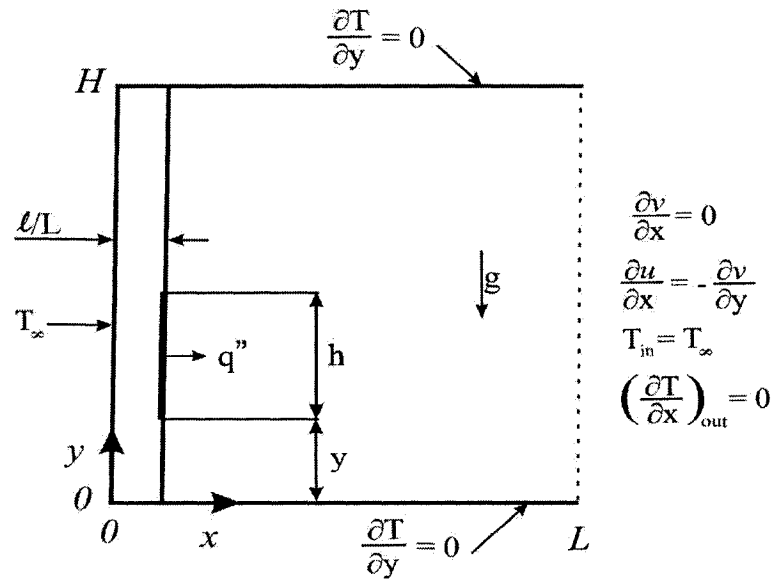

Figure 1.2: Schematic of the cavity with a conductive wall, a discrete heater, the coordinate system and boundary conditions.

We present this M.Sc.A. thesis in 4 chapters, including Chapter 1 for introduction and literature review. We will present in Chapter 2, problem definition, mathematical model and governing equations of mass, momentum and energy conservation with boundary conditions, as well as numerical method, code verification, and grid independence study. We will present in Chapter 3, the results obtained and discussion on the square cavity with finite number of discrete heaters in their optimum positions, and in Chapter 4, those on the cavities with conductive wall and a single discrete heater at its optimum position. Finally, we will present general conclusions in Chapter 5.

CHAPTER 2

PROBLEM AND MATHEMATICAL MODEL

2.1. Problems

2.1.1. Open Cavities without Massive Wall and with Finite Number of Discrete Heaters

The problem is to determine the optimum position of one, two or more discrete heating elements in an open square cavity, cooled by natural convection. Further, heat transfer performance of each case is studied using the determined optimum positions.

Schematic of the two dimensional open square cavity with three discrete heating elements case and the boundary conditions are shown in Fig. 1.1. All three solid boundaries of the cavity are adiabatic and the side facing the vertical left boundary is open to ambient air. One, two or three discrete heating elements are installed on the vertical left boundary. Each heating element of height h and coordinate $(0, y_i)$ dissipates heat at constant heat flux, $q"$. The cooling air from a reservoir enters the cavity through the lower part of the opening; it circulates along the heating elements and exits from the upper part of the opening.

2.1.2. Open Cavities with Massive Wall and a Single Discrete Heater

First, we determine the optimum position of a discrete heating element in open cavities installed on a conducting wall facing the opening, cooled by natural convection. Second, we study heat transfer performance of each case using the heater at its optimum position and carry out a sensitivity study on the governing parameters.

Schematic of the two dimensional open square cavity with a discrete heating element and the boundary conditions are shown in Fig. 1.2. Horizontal boundaries of the cavity are adiabatic, the left face of the solid wall is isothermal and its right side is in the open cavity in contact with the ambient air. A discrete heating element is installed on the solid wall inside the cavity. The heating element of height h and coordinate $(0, y_i)$ dissipates heat at constant heat flux, $q"$. The cooling air from a reservoir enters the cavity through the lower part of the opening; it circulates along the heating element and exits from the upper part of the opening.

2.2. Mathematical Model

We assume that the fluid is Newtonian, the radiation is negligible and the third dimension has a negligible effect on the flow and heat transfer. With these assumptions, we use two dimensional conservation equations for mass, momentum and energy with Bussinesq approximation. By using L as the length scale, α/L as the velocity scale,

Lq''/k as the temperature scale and L^2/α for the time scale, we obtain following non-dimensional equations

Mass conservation:

$$\frac{\partial U}{\partial X}+\frac{\partial V}{\partial Y}=0 \tag{1}$$

Momentum equation in x direction:

$$\frac{\partial U}{\partial \tau}+U\frac{\partial U}{\partial X}+V\frac{\partial U}{\partial Y}=-\frac{\partial P}{\partial X}+\Gamma \,\mathrm{Pr}\,\nabla^2 U \tag{2}$$

Momentum equation in y direction:

$$\frac{\partial V}{\partial \tau}+U\frac{\partial V}{\partial Y}+V\frac{\partial V}{\partial Y}=-\frac{\partial P}{\partial Y}+\Gamma \,\mathrm{Pr}\,\nabla^2 V+Ra\,\mathrm{Pr}\,\theta \tag{3}$$

Energy equation:

$$\frac{\partial \theta}{\partial \tau}+U\frac{\partial \theta}{\partial X}+V\frac{\partial \theta}{\partial Y}=k_r\nabla^2\theta \tag{4}$$

where Γ is a general diffusion coefficient and equal to 1 in the fluid region and equal to 10^{15} in the solid region, k_r is 1 in the fluid region and k_s/k_f in the solid region. The terms Γ is introduced in the equations to ensure $U=V=0$ everywhere including at the solid-fluid interface and k_r is used to account conduction in the solid region. For the case of open cavity without massive wall, Γ and k_r are taken equal to 1 in the computation domain.

The governing parameters are $Ra = g\beta q'' L^4/(\upsilon\alpha k)$ and $Pr = \upsilon/\alpha$, and A, h/L and in case of open cavity with a massive wall A, k_r and ℓ/L.

The average and normalized Nusselt numbers are calculated as

$$\overline{Nu} = \frac{-\int_0^A \frac{\partial\theta}{\partial X} dY}{\int_0^A (\theta_1 - \theta_2)} \tag{5}$$

$$Nu = \frac{\overline{Nu}_{Ra}}{\overline{Nu}_{Ra=0}} \tag{6}$$

The volume flow rate, $\dot{V}$ is calculated as:

$$\dot{V} = -\int_{X=1} U_{in} dY \tag{7}$$

where $U_{in} = U_{X=1}$ if $U_{X=1} < 0$ and $U_{in} = 0$ if $U_{X=1} \geq 0$

The stream function is calculated from its definition as:

$$U = -\frac{\partial\psi}{\partial Y}, \quad V = \frac{\partial\psi}{\partial X} \tag{8}$$

ψ is zero on the solid surfaces and the streamlines are drawn by $\Delta\psi = (\psi_{max} - \psi_{min})/n$ with n is the number of increments.

The conductance is used instead of the Nusselt number for numerical convenience in the optimization study. It is calculated as:

$$C = \frac{Q'}{k(T_{max} - T_\infty)} = \frac{\int_y^{y+h} q'' dy}{k(T_{max} - T_\infty)} = \frac{q'' \int_y^{y+h} dy}{\theta_{max} q'' L} = \frac{h/L}{\theta_{max}} \tag{9}$$

2.2.1. Boundary Conditions

2.2.1.1. Open Cavities without Massive Wall

Boundary conditions are:

On solid surfaces: $U = 0, V = 0$ (10)

On adiabatic walls: $\frac{\partial \theta}{\partial n} = 0$ (11)

On the heaters: $q = \frac{\partial \theta}{\partial X} = 1$ (12)

At the opening: $\frac{\partial V}{\partial X} = 0, \frac{\partial U}{\partial X} = -\frac{\partial V}{\partial Y}, \theta_{in} = 0, \left(\frac{\partial \theta}{\partial X}\right)_{out} = 0$ (13)

We note that when the fluid flows into the cavity, $\theta_{in} = 0$ and when it flows out of the cavity, $\left(\frac{\partial \theta}{\partial X}\right)_{out} = 0$.

2.2.1.2. Open Cavities with Massive Wall

Boundary conditions are:

On solid surfaces: $U = 0, V = 0$ (14)

X=0 to 1, Y=0 and A: $\frac{\partial \theta}{\partial n} = 0$ (15)

X=0, Y=0 to A: $\theta = 0$ (16)

X=1, Y=0 to A: $\frac{\partial V}{\partial X} = 0, \frac{\partial U}{\partial X} = -\frac{\partial V}{\partial Y}, \theta_{in} = 0, \left(\frac{\partial \theta}{\partial X}\right)_{out} = 0$ (17)

On the heater: $q = \frac{\partial \theta}{\partial X} = 1$ (18)

The remark made for the temperature boundary condition in Eq. (13) applies also for the temperature boundary condition in Eq. (17). We note that with the assumptions of negligible radiation and conduction through the fluid, the boundary condition at the opening, Eqs. (13) or (17) is shown to be satisfactory for the case of computation domain confined to the open cavity [13].

2.3. Numerical Technique

The numerical method used to solve Eqs. (1) to (4) with the boundary conditions Eqs. (10) to (13) for case of without a massive wall and Eqs. (14) to (18) for case of with a massive wall is the SIMPLER (Semi-Implicit Method for Pressure Linked Equations Revised) algorithm [14]. The computer code based on the mathematical formulation presented above and the SIMPLER method is validated with respect to the benchmark [15]. The results of validation are shown in Table 2.1. We see that the deviations in Nusselt numbers at all Rayleigh numbers of interest are good and with acceptable deviation, the concordance is excellent. In addition, the average Nusselt numbers at the hot and cold walls were compared, which showed a maximum difference of about 0.5%

in all runs. The present code is tested also to simulate the case studied by Chan and Tien [10] with enlarged computational domain. We used restricted computational domain and compared the results with theirs with extended computational domain. The results are shown in Table 2.2. It is noted that in restricted domain case, the deviation is higher at $Ra=10^7$, because the flow simulation at the cavity corners is not perfect. Despite this, the approximation made is acceptable.

Table 2.1: Comparison of the benchmark results [15] at $x = 0$ and $x= 1/2$ plane.

		[15]	This Study	
Ra	Mesh Number	*Nu*_0 / *Nu*_1/2	*Nu*_0 / *Nu*_1/2	% Deviations
10^3	41x41	1.116 / 1.117	1.1192 / 1.1192	0.28 / 0.19
10^4	41x41	2.242 / 2.242	2.2597 / 2.2597	0.78 / 0.78
10^5	81x81	4.523 / 4.523	4.5472 / 4.5472	0.53 / 0.53
10^6	81x81	8.928 / 8.928	8.9799 / 8.9799	0.58 / 0.58

Table 2.2: Comparison of the results with the enlarged domain [10] and the cavity restricted domain used in this study.

Ra	$Nu/\dot{V}$ [10]	$Nu/\dot{V}$ [this study]	% Deviations
10^5	7.69/21.10	7.81/22.65	-1.56/-7.34
10^6	15.00/47.30	15.23/47.02	-1.53/+0.59
10^7	28.60/96.00	29.86/94.15	-4.41/+1.93

Uniform grids in X and Y direction were used for all computations. Grid convergence was studied for the case of $A = 1$ with grid sizes from 21x21 to 151x151 at $Ra = 10^5$ and

10^7. The results for open cavity without and with solid wall are presented in Tables 2.3 and 2.4.

For the cavity without solid wall, using 81x81 and 101x101, the variations in *Nu* and *C* are $6.2\text{x}10^{-4}$ and $1.27\text{x}10^{-2}$, respectively at $Ra=10^5$, and they are $2.1\text{x}10^{-3}$ and $1.3\text{x}10^{-2}$, respectively at $Ra=10^7$, as shown in Table 2.3. Hence, we made a compromise between computation time and precision, and selected the grid size of 81x81. Using a system with a processor of 3.2 GHz clock speed, for 81x81 grid size, at $Ra=10^6$, the typical execution time was 92 s for single heater case and 76 s for three heaters case.

For the cavity with solid wall, the grid convergence was studied for the case of square cavity having $\ell/L = 0.10$ and $k_r = 10$ with grid sizes from 21x21 to 101x101 at $Ra = 10^8$ and 10^{10}. The results are presented in Table 2.4. We see, for example, at $Ra = 10^{10}$ that between 31x31 and 61x61, the variation in Nusselt is 0.59%, it is 0.57% in volume flow rate, and 0.28% in conductance. Thus, 31x31 grid size was a good choice from the computation time and precision point of view for the square cavity. We conducted similar tests with the shallow and tall cavities and used 61x31 for $A = 0.5$ and 31x61 for $A = 2$ grid sizes. The grid size in the wall was 5, 10 and 15 in the X direction for the wall thickness of $\ell/L = 0.05$, 0.10 and 0.15 respectively, and the rest were in the cavity. Using the same computer as for the cavity without solid wall, for $A = 1$, with 31x31 grid size, at $Ra=10^{10}$, the typical execution time was 112 s.

Table 2.3: Grid independence study results with $A = 1$ at $Ra = 10^5$ and 10^7.

Size		21x21	41x41	61x61	81x81	101x101	151x151
$Ra = 10^5$	Nu	3.323	3.223	3.211	3.206	3.204	3.201
	C	0.818	0.940	0.985	1.008	1.021	1.039
$Ra = 10^7$	Nu	6.973	6.918	6.831	6.800	6.786	6.773
	C	1.287	1.592	1.672	1.709	1.733	1.766

Table 2.4: Grid independence study results with A=1, ΔL =0.10, k_r =10

Size		21x21	31x31	61x61	101x101
$Ra = 10^8$	Nu	3.227	3.111	3.103	3.077
	V	5.855	5.557	5.567	5.455
	C	3521.540	3546.938	3582.945	3597.985
$Ra = 10^{10}$	Nu	13.159	12.140	12.069	11.775
	V	24.382	29.913	29.743	29.256
	C	4125.980	3964.059	3953.611	3953.611

A converged solution was obtained by iterating in time until variations in the primitive variables between subsequent time steps were:

$$\sum(\phi_{i,j}^{old} - \phi_{i,j}) < 10^{-4} \tag{19}$$

where ϕ stands for U, V, and θ.

Within the same time step, the residual of the pressure term was less than 10^{-3} [14]. In addition, the accuracy of the solution was double-checked using the energy conservation on the domain to ensure it was less than 10^{-4}.

CHAPTER 3

NATURAL CONVECTION IN AN OPEN SQUARE CAVITY WITH DISCRETE HEATERS AT THEIR OPTIMIZED POSITIONS

3.1. Introduction

The problem description, mathematical model and boundary conditions for this study have been presented in Chapter 2. This study and the results are submitted for publication [16]. We present in section 3.2, the optimization study results, in section 3.3, the parametric study results obtained with the discrete heating elements at their optimum positions, and in section 3.4, the main conclusions of this study. The aspect ratio was, A=1 and kept constant. The variable parameters considered are dimensionless height of heating element, h/L = 0.05, 0.10 and 0.20, number of heating elements, N = 1, 2 and 3, and Rayleigh number, Ra = 10^3 to 10^7. Prandtl number, Pr = 0.70 for air was kept constant.

3.2 Optimization Study

It was carried out to obtain the optimum position of heating elements by taking the number of heaters and their size constant, and by varying their positions. The procedure was as follows: (i) We compute conductance $C(Y)$ for a given N and h/L, at a constant

Ra, (ii) we determine the maximum conduction, C_{max} at its optimum position Y_{opt}. (iii) We repeat the steps (i) and (ii) to determine C(*Y*), C_{max} and Y_{opt} at all the other Rayleigh numbers, from 10^3 to 10^7, while keeping *N* and *h/L* the same. (iv) We repeat the steps (i) and (iii) to obtain the maximum conductance at its optimum position, $C_{max}(Y_{opt})$ for the same number of heater, *N* but different heater sizes, *h/L*. Then, we repeat the steps (i) – (iv) to obtain the maximum conductance at its optimum position, $C_{max}(Y_{opt})$ for different number of heaters, *N*. With the variable parameters considered above, for each heater size, we had 80 computations for *N*=1, 250 for *N*=2 and 190 for *N*=3. For three heater sizes, we had all together about 1500 computations to determine the optimum positions of the cases studied.

Typical results to obtain the conductance *C*(*Y*) for *N*=1, *h/L*=0.10, *Ra* =10^3, 10^5 and 10^7 are presented in Fig. 3.1(a). We can make several observations: (i) For all the Rayleigh numbers, the conductance changes with the position of the heater. We have smaller conductance at the lowest position when the heater is at the bottom; the conductance is increasing gradually as its position is raised reaching a maximum around mid-height and it is decreasing thereafter to another low conductance at the top position. This is expected since the cold air enters the cavity from the bottom, flows over the lower horizontal boundary and turns around before reaching the vertical side; hence, the conductance is lower near the bottom corner. As the heater is positioned higher, the incoming cold air flows over it; its conductance increases and reaches its maximum value at its optimum position.

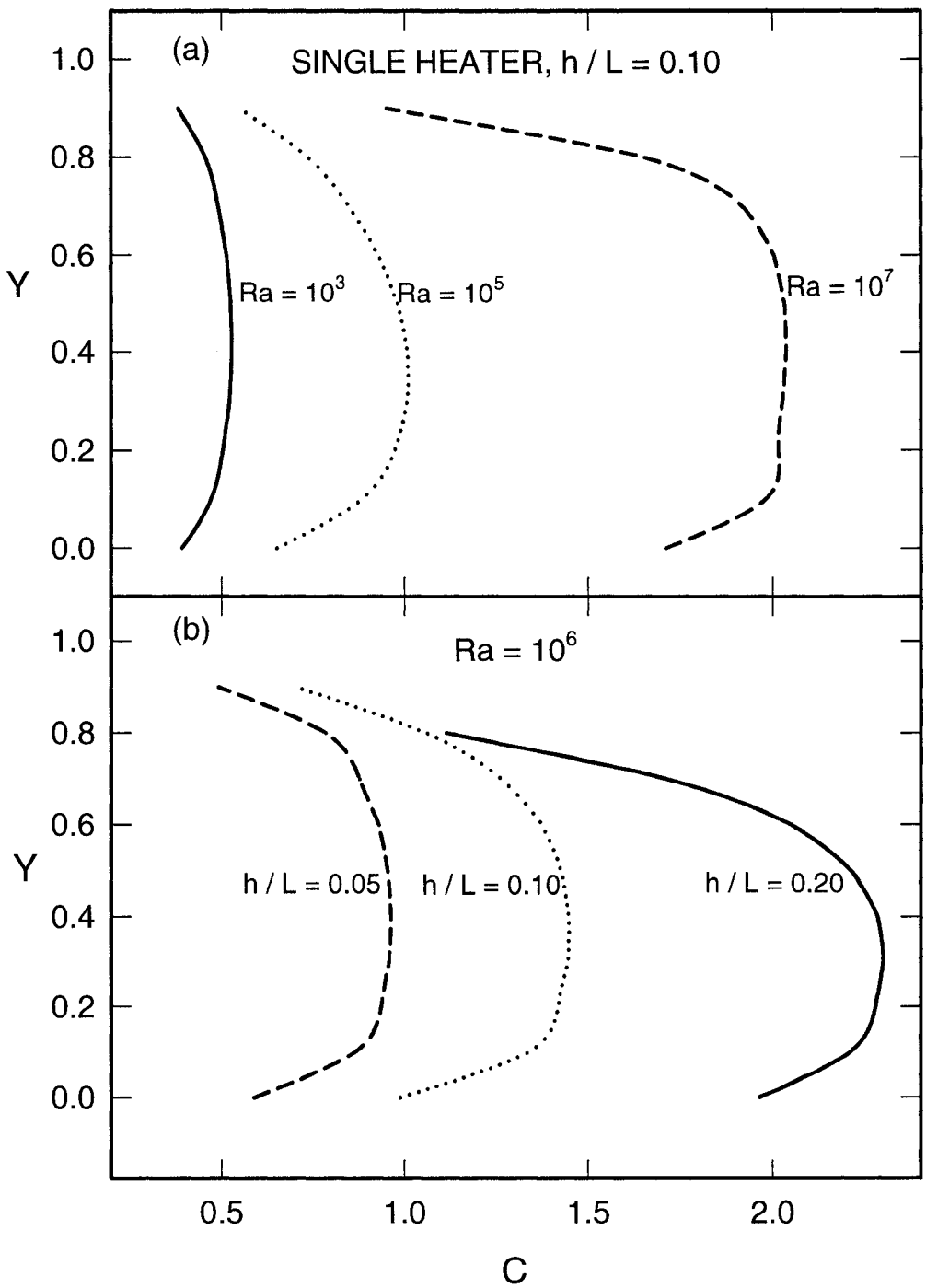

Figure 3.1: The maximization of the global conductance when only one heat source is present

At the near top position, the air flow is again turned away from the heater to follow the top horizontal boundary and exit the cavity; hence the conductance is again relatively lower. (ii) For all cases, we see broad maxima, though using the computation results or changing scale of conductance, it is not difficult to identify C_{max} at its Y_{opt}. (iii) As the Rayleigh number is increased, the air flow as well as the conductance is increased. Following the increased air flow rate and resulting streamlines, the conductance, $C(Y)$ is increased accordingly. Indeed, ψ_{ext} and θ_{max} are -0.414 and 0.1905 at $Ra=10^3$, -5.4799 and 0.1019 at $Ra=10^5$ and -18.9763 and 0.0492 at $Ra=10^7$. They show that as Ra is increased, the circulation is increased and the maximum temperature is decreased, which is an expected result.

The effect of the heater size for $Ra=10^6$ is presented in Fig. 3.1(b) for h/L=0.05, 0.10 and 0.20. We see that the conductance is strongly affected by the heater size. In fact, ψ_{ext} and θ_{max} are both increasing functions of the heater size. For example, at Y=0.5, ψ_{ext} and θ_{max} are -9.0116 and 0.0524 for h/L=0.05, -10.7295 and 0.0701 for h/L=0.10 and -12.4927 and 0.0904 for h/L=0.20. Thus, the conductance calculated by Eq. 9 is C=0.95, 1.43 and 2.21 for h/L=0.05, 0.10 and 0.20 respectively.

We present streamlines and isotherms in Fig. 3.2 for the cases corresponding to Fig. 3.1(a) at $Ra=10^3$, 10^5 and 10^7. The heater size is h/L=0.10 and its two positions are shown, the upper figures at the bottom, Y=0 and the lower ones are at the optimum position, Y_{opt}=0.4.

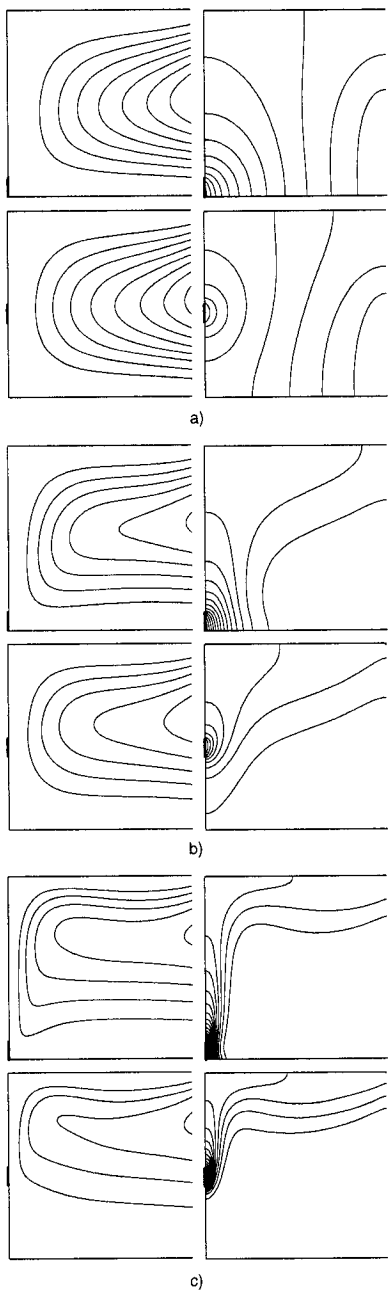

Figure 3.2: Streamlines (on the left) and isotherms (on the right) for h/L=0.10, the most lower heater position (the upper figure), the optimum heater position (the lower figure, (a) Ra=10^3, Y_{opt} (the upper and lower figure) = 0.0 and 0.41, (b) Ra=10^5, Y_{opt} (the upper and lower figure) = 0.0 and 0.39, (c) Ra=10^7, Y_{opt} (the upper and lower figure) = 0.0 and 0.38.

We observe in Fig. 3.2(a) at $Ra=10^3$ that the heat transfer is conduction dominated and the flow in both cases is almost similar, the flow is affected by the heater and it is slightly non-symmetric. ψ_{ext} and θ_{max} for $Ra=10^3$ are -0.3992 and 0.2547 at $Y=0$ and -0.4141 and 0.1895 at $Y=Y_{opt}$. It is seen that the heater at its optimum position is better cooled by the inflowing air. At $Ra=10^5$ in Fig. 3.2(b), ψ_{ext} and θ_{max} are -6.1484 and 0.1538 at $Y=0$ and -5.6808 and 0.0992 at $Y=Y_{opt}$. Again, the cooling is better at $Y=Y_{opt}$ position. Finally, at $Ra=10^7$ in Fig. 3.2(c), ψ_{ext} and θ_{max} are -25.7182 and 0.0585 at $Y=0$ and -20.5515 and 0.0491 at $Y=Y_{opt}$. Once again, the cooling is better at $Y=Y_{opt}$. Thus, Fig. 3.2 shows that our observations regarding Fig. 3.1(a) are confirmed.

We present in Fig. 3.3 (a) and (b) the optimum heater position Y_{opt} and the maximum conductance C_{max} as a function of the Rayleigh number for a single heater having h/L=0.05, 0.10 and 0.20. We see in Fig. 3.3(a) that generally, the optimum position is slightly decreasing function of the Rayleigh number; this is expected since for increasing Ra, the circulation increases at the lower half of the cavity and the optimum heater position is at slightly lower level. We see also that Y_{opt} is at a lower position as the heater size is increased, as observed earlier in Fig. 3.1. We see in Fig. 3.3(b) that the maximum conductance C_{max} is an increasing function of the Rayleigh number, as observed in Fig. 3.1(a). C_{max} is an increasing function of heater size, as a consequence of our observations in Fig. 3.1(b). The results of Fig. 3.3 show that the optimum position of a single heater is at the lower half of the open cavity and not at the center. The conductance is maximized by lowering Y_{opt} slightly as the Rayleigh number is increased.

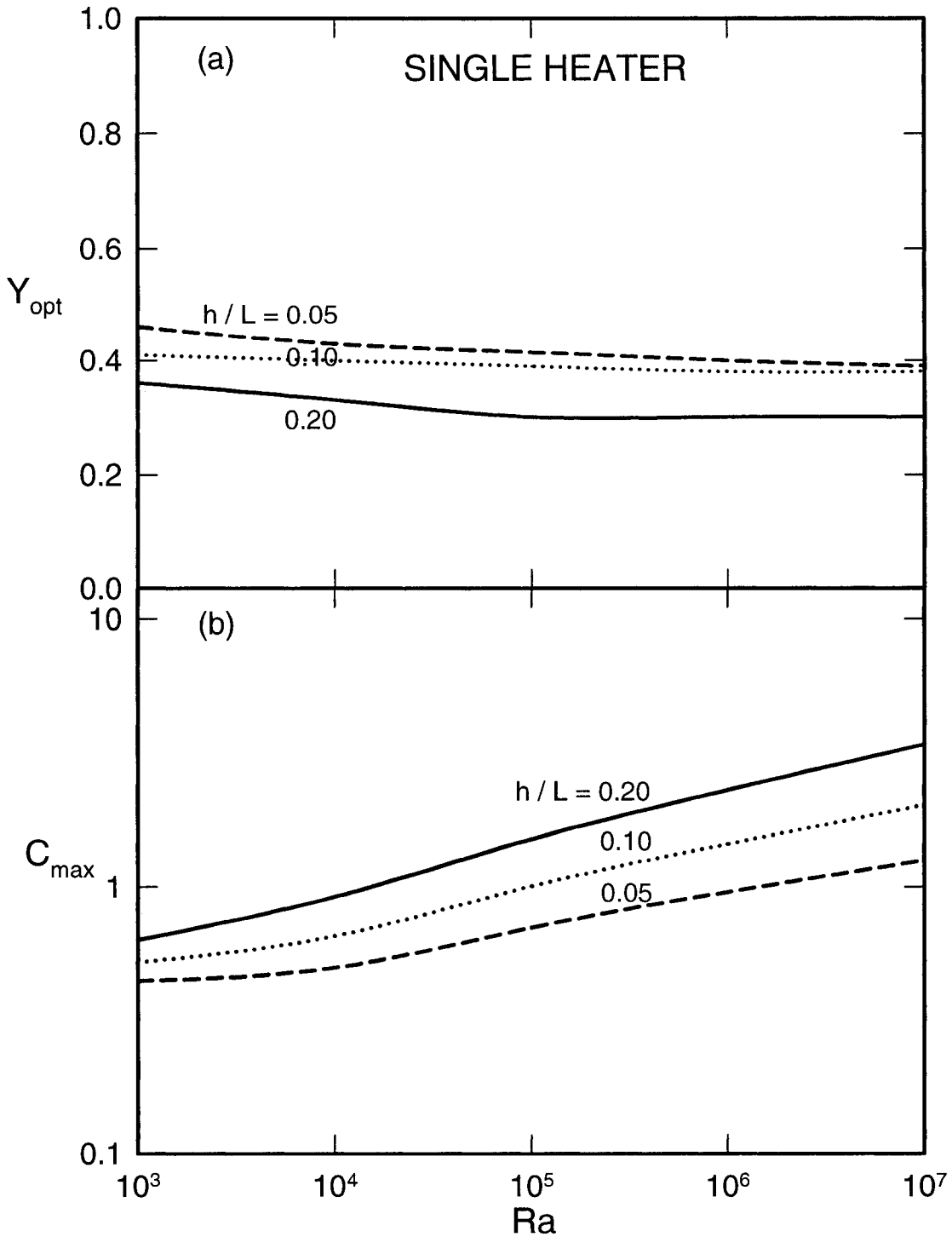

Figure 3.3: (a) The optimal heater location and (b) corresponding maximum global conductance as a function of the Rayleigh number for the single heat source.

Following the procedure outlined earlier, we studied the cases with two heaters and three heaters. For two heaters case, the optimum position Y_{opt} is determined by searching the best position of the second heater while keeping the first at a fixed position and then repeating this procedure until all position combinations are obtained. As a result, the global maximum conductance C_{max} for the two heaters is found. The results are shown in Fig. 3.4. We see in Fig. 3.4(a) that the trends for both heaters are similar to the case of the single heater, i.e., Y_{opt} is a decreasing function of the Rayleigh for the same reason as explained earlier. Compared to the single heater case of Fig. 3.3, the first heater is at a lower level position and the second heater is at a higher level. We see in Fig. 3.4(b) that C_{max} is an increasing function of the Rayleigh as well as of h/L. Compared to a single heater case, we notice that C_{max} is generally increased since it is the global maximum conductance comprising two heaters.

We present the results with three heaters in Fig. 3.5. It appears in Fig. 3.5(a) that the optimum position Y_{opt} is again a decreasing function of Ra from 10^3 to 10^7 and also, it is a strong function of h/L from 0.05 to 0.20. We make similar observations regarding the positions of the heaters: when compared to the single and the two heaters cases, the first heater is at the lowest position and the third heater at the highest position. The maximum global conductance C_{max} presented in Fig. 3.5(b) is then function of the Rayleigh number and heater size, h/L. As in the previous two cases, the maximum global conductance is an increasing function of the Rayleigh number and also of the heater size h/L.

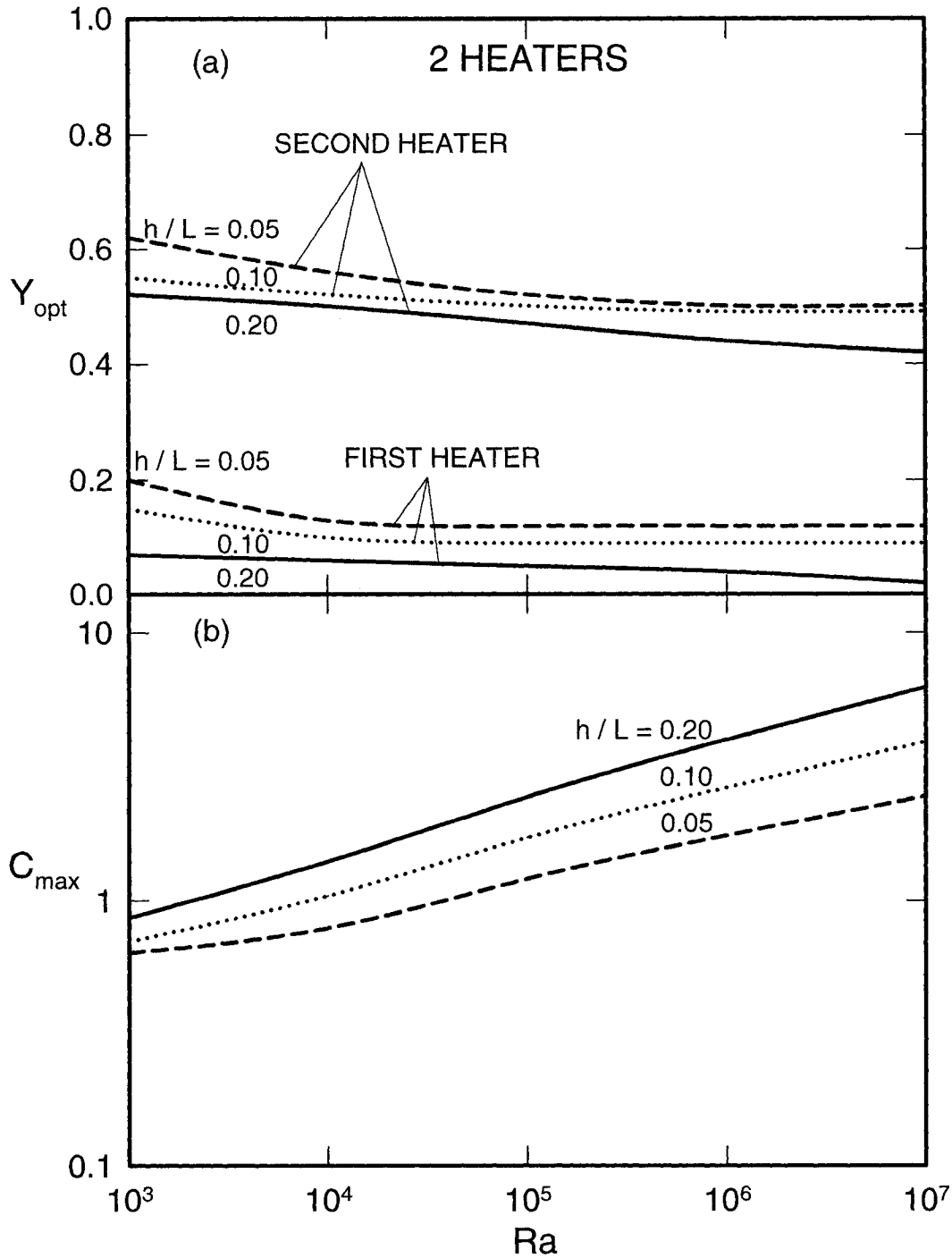

Figure 3.4: (a) The optimal heater location and (b) corresponding maximum global conductance as a function of the Rayleigh number for two heat sources.

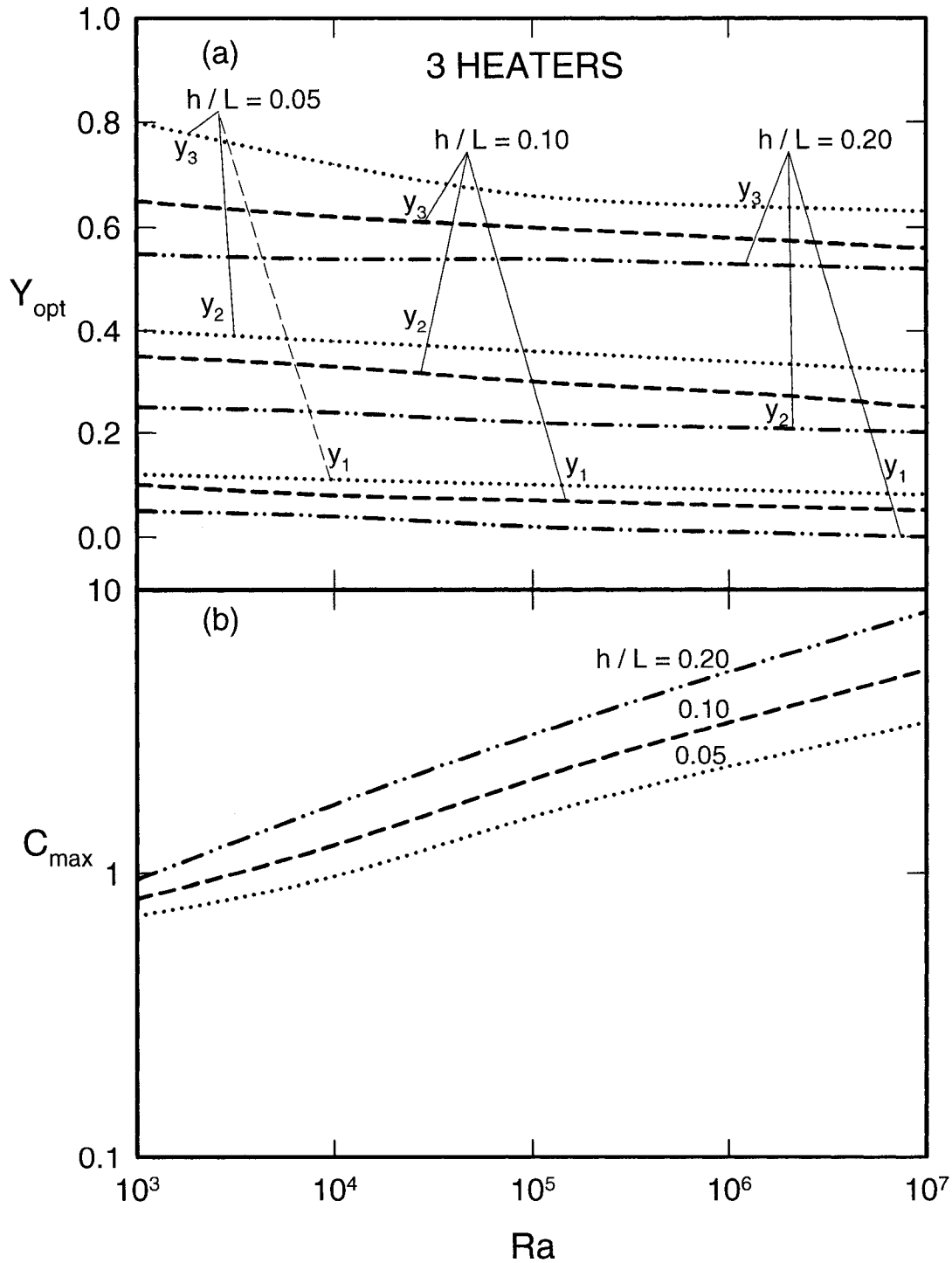

Figure 3.5: (a) The optimal heater location and (b) corresponding maximum global conductance as a function of the Rayleigh number for three heat sources.

We note also that the maximum global conductance C_{max} is increased with respect to the case of the two heaters of Fig. 3.4(b).

In comparison with the square enclosure case having N=1, 2 and 3 [3], it is noted that the heater positions and distances between them have the expected trend at low Rayleigh numbers, a conduction dominated regime. At $Ra = 10^3$ for example, we compared the conductance results for $h/L = 0.10$ of Fig. 3 of [3] and found that the conductance in the open cavity was lower by 14.5%, thus showing that the cooling of the heater is quite different. Indeed, Y_{opt} in the open cavity case is lower by 2.1%, 9.8% and 8.3% for h/L = 0.05, 0.10 and 0.20 respectively. At high Rayleigh numbers, the heaters in the open cavity case are positioned at higher levels, although the overall positioning are similar: at $Ra = 10^6$ for example, Y_{opt} in the open cavity is positioned higher by 17.6%, 31% and 20% for h/L = 0.05, 0.10 and 0.20 respectively. In fact, the comparative iso-lines (not presented here) showed that the flow and temperature fields were quite different for enclosure and open cavity, particularly at high Rayleigh numbers. For example, at Ra = 10^6, in the enclosure case, ψ_{ext}/θ_{max} = -7.4873 (X=0.4125, Y=0.5730)/0.079 and in the open cavity case, ψ_{ext}/θ_{max} = -11.5362 (X=1.00, Y=0.6620)/0.069; the isotherms in the latter case showed that the temperature gradient was higher near the heater, thus heat transfer and cooling were more vigorous. The flow rate at the mid-plane (X=0.5) of the enclosure and that at the exit plane of the open cavity are also quite different: $\dot{V}$ (enclosure)/ $\dot{V}$ (open cavity) are 0.1363/0.2198 and 7.4345/11.5362 at $Ra = 10^3$ and 10^6 respectively. This is expected since the ambient air into the open cavity flows

through the lower 2/3 part of the opening. In contrast, the air in the enclosure circulates close to the bottom wall, as a result of which the first heater's optimum position is closer to the bottom. We see that the flow and temperature fields in the enclosure and cavity cases are quite different. Thus, optimum positions are different, although some similarities exist, as they should.

3.3. Heat Transfer and Volume Flow Rate

The average normalized Nusselt number by Eq. (6) and the volume flow rate $\dot{V}$ by Eq. (7) are calculated and presented in Figs. 3.6 to 3.8 for the three cases of one, two and three heaters. The results are presented for the case of optimum positions, i.e. for the maximized conductance of each heater.

We present the case of single heater in Fig. 3.6. We see in Fig. 3.6(a) that *Nu* is an increasing function of *Ra* and *h/L*. At low Rayleigh numbers, the heat transfer is conduction dominated; *Nu* is equal to one for all three heater sizes. As *Ra* is increased the convection becomes dominant and we can see that *Nu* becomes an increasing function of the heater size *h/L*. The volume flow rate $\dot{V}$ as a function of *Ra* with *h/L* as a parameter is shown in Fig. 3.6(b). As expected, $\dot{V}$ is an increasing function of both *Ra* and *h/L*.

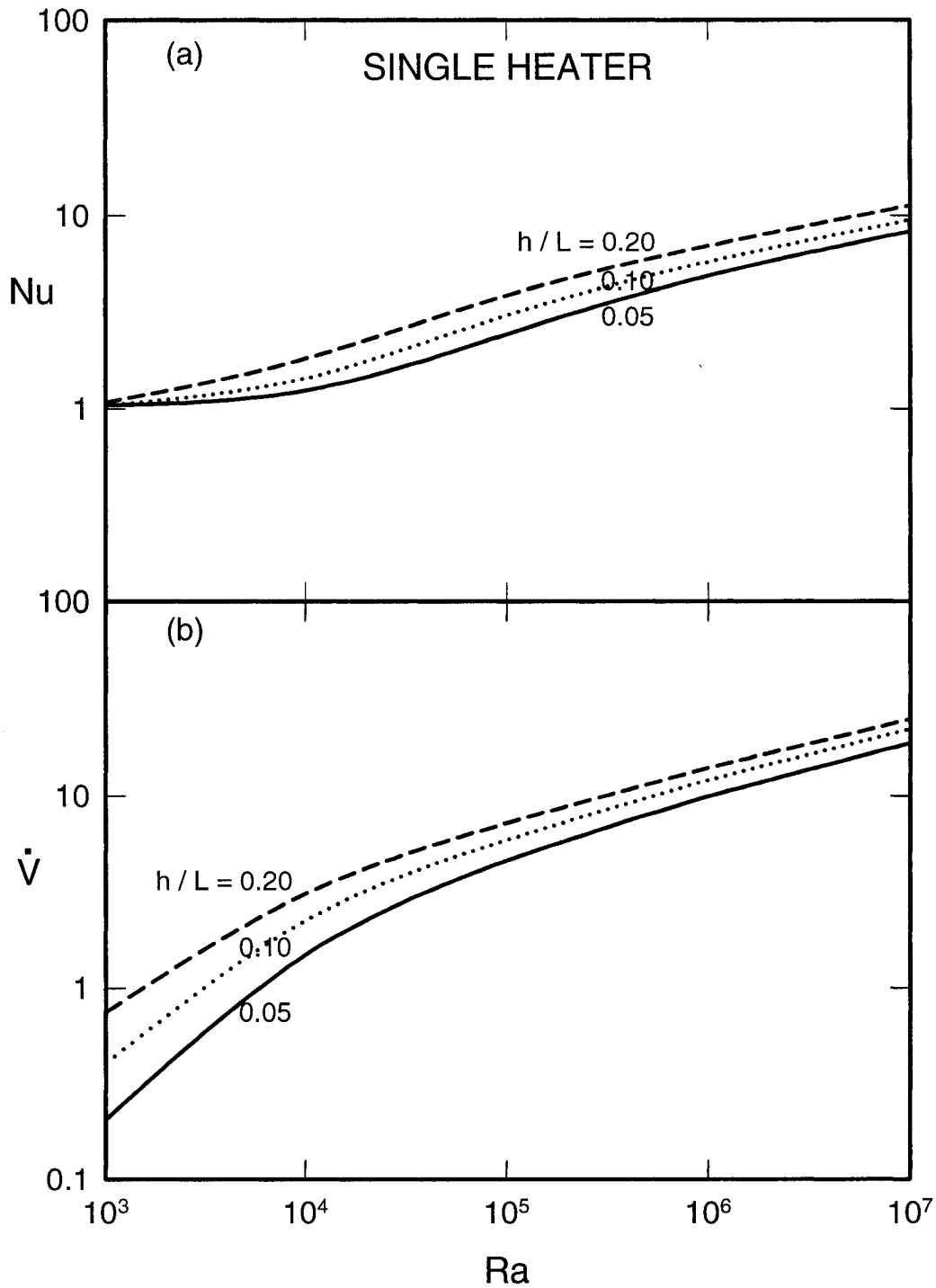

Figure 3.6: (a) Nusselt number and (b) flow rate as a function of the Rayleigh number for the single heat source of three sizes.

The case with the two heaters is shown in Fig. 3.7, which shows that the heat transfer is conduction dominated at $Ra=10^3$, thereafter it becomes convection dominated. Nu is an increasing function of Ra and h/L.

Compared to the single heater case for h/L from 0.05 to 0.20, Nu is increased by 15.6 to 7.8% respectively at $Ra=10^7$ due to increased number of heaters. The volume flow rate $\dot{V}$ is also an increasing function of Ra and h/L. Compared to the single heater case for h/L from 0.05 to 0.20, it is increased respectively by 91.8 to 67% at $Ra=10^3$ and 15 to 24.4% at $Ra=10^7$. The case with three heaters is shown in Fig. 3.8. In this case also, both Nu and $\dot{V}$ are an increasing function of Ra and h/L. Fig.3.8(a) shows that the heat transfer is in conduction regime at $Ra=10^3$, thereafter it becomes convection dominated. Compared to the single heater case for h/L from 0.05 to 0.20, Nu is increased by 19.2 to 9.5% at $Ra=10^7$. The flow rate $\dot{V}$ is increased by 1.77 to 1.17 times at $Ra=10^3$ and by 29.9 to 40.9% at $Ra=10^7$. Obviously, the changes of Nu and $\dot{V}$ are due to increased number of heaters.

To see the reason for increased heat transfer and volume flow rate with increasing heater number, the streamlines and isotherms for the case of $h/L=0.10$ and $Ra=10^6$ with one, two and three heaters at their optimum positions are produced and shown in Fig. 3.9. ψ_{ext} and θ_{max} are -11.4124 ($X=1$, $Y=0.6625$) and 0.0691 respectively for the single heater case in Fig. 3.9(a).

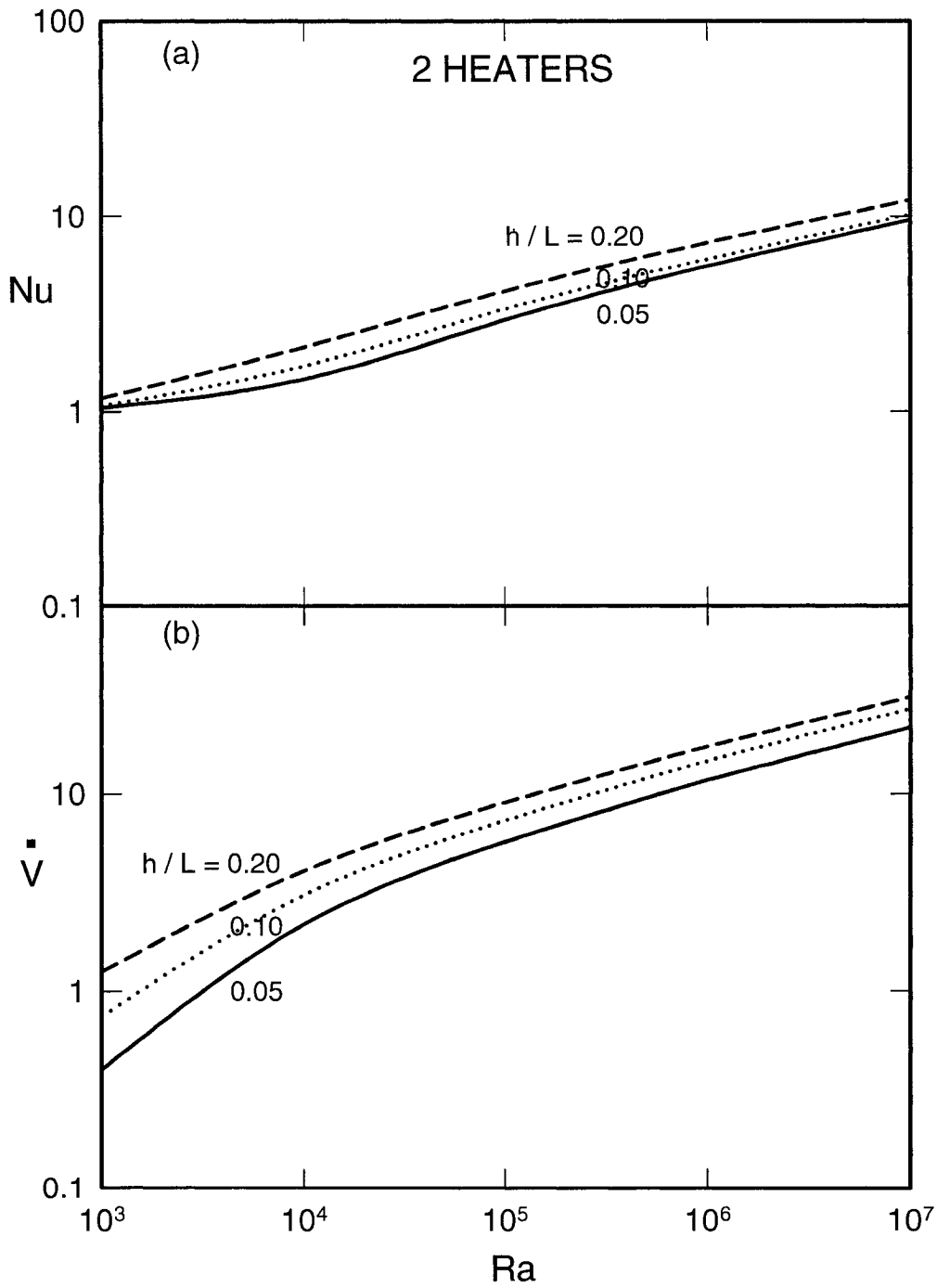

Figure 3.7: (a) Nusselt number and (b) flow rate as a function of the Rayleigh number for the two heat sources of three sizes.

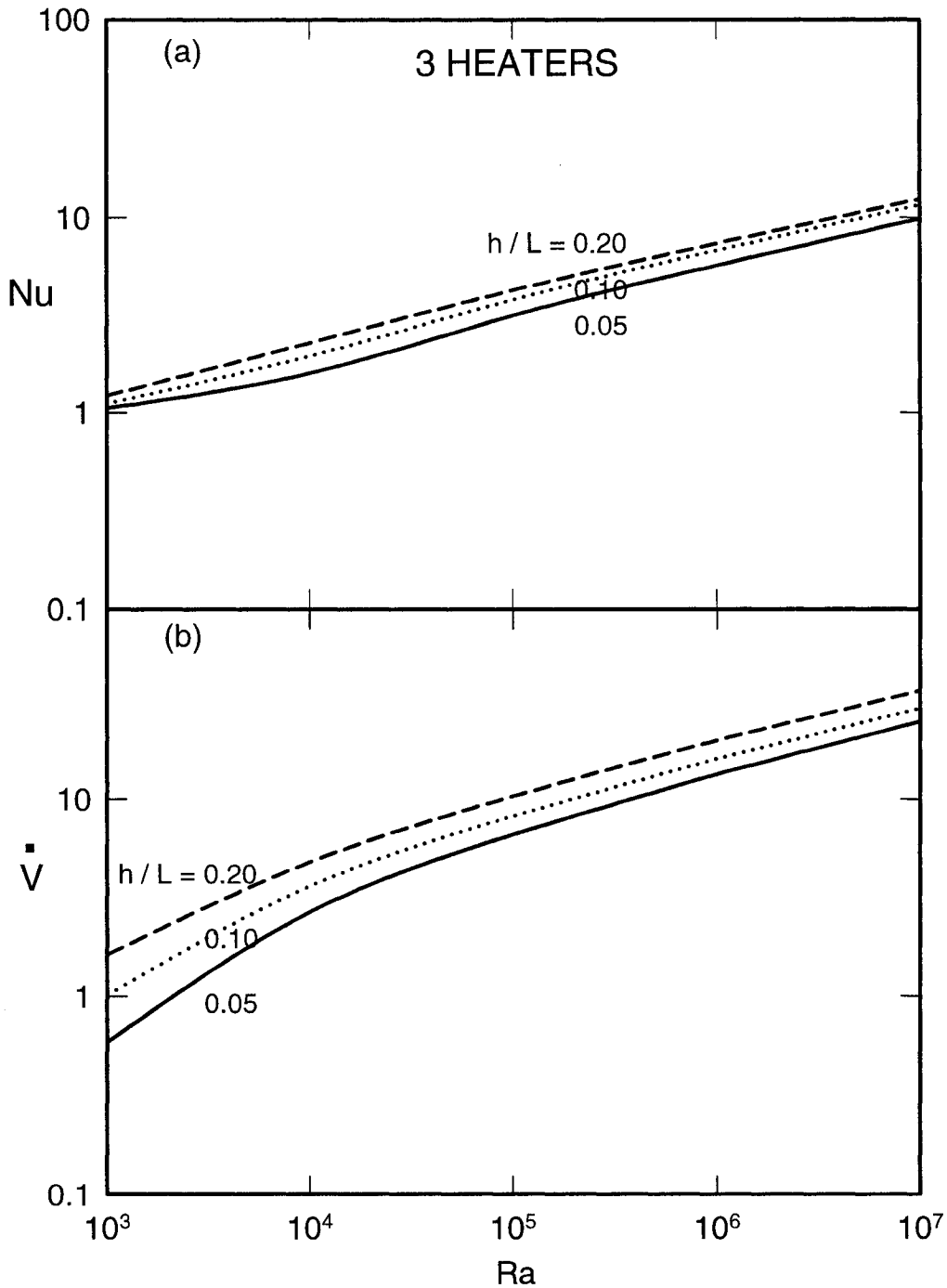

Figure 3.8: (a) Nusselt number and (b) flow rate as a function of the Rayleigh number for the three heat sources of three sizes.

It is clearly seen that the heater is positioned at off center, at slightly lower part of the enclosure. The flow enters and moves upward following the position of the heater and flows over the vertical wall and top horizontal wall and exit as a jet. The cold ambient air enters at lower 2/3 of the opening section and the hot air exits at upper 1/3. The isotherms shown on the right hand side follow this trend as a consequence of which the air is cold in about 2/3 part of the cavity. For the two heater case in Fig. 3.4(a), the heaters are positioned with unequal distances from the enclosure bottom to the first heater and from the first to the second heater. ψ_{ext} and θ_{max} are -14.7678 (X=1, Y=0.6714) and 0.0755 respectively. The strength of circulation is increased with respect to the single heater case.

Since the optimum position of the first heater is at the lower part of the enclosure, the cold air enters and follows the bottom horizontal wall, heated at first by the first heater and then by the second, it flows over the whole vertical wall and exits following the top horizontal wall. The ambient air entrance section in this case is increased to 67.14% of the opening, which is little larger than 2/3. The isotherms shown on the right hand side of Fig. 3.9(b) depict clearly the domain of the cold air, which occupies the lower half of the enclosure. Compared to the single heater case, the air is heated by the first heater when the air reaches the vertical wall. Then by the second heater; then the air continues to go up, parallel to the vertical wall. The three heater case is shown in Fig. 3.9(c).

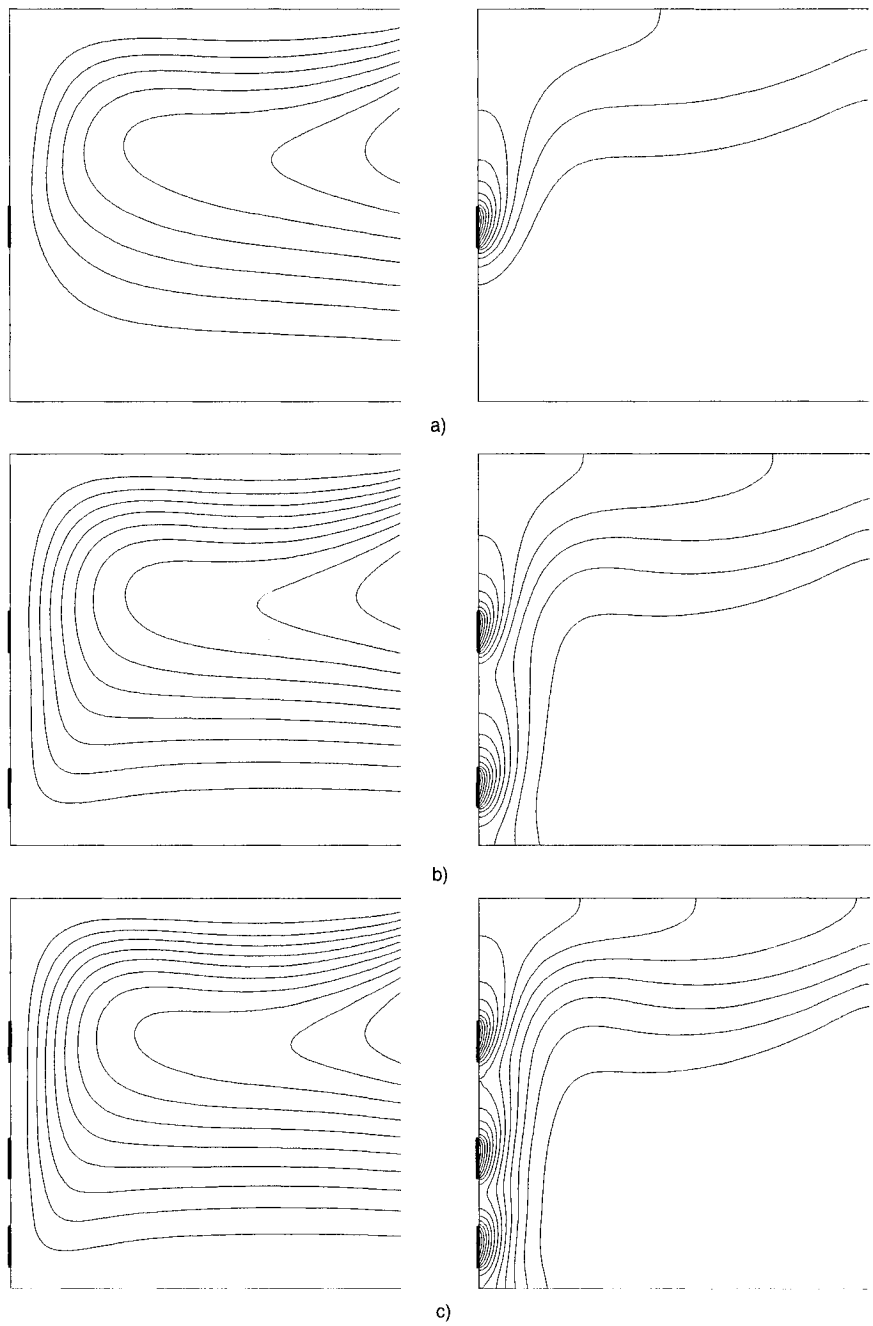

Figure 3.9: Streamlines (on the left) and isotherms (on the right) with h/L=0.10 and Ra=10^6. (a) One heater at its optimum position, Y_{opt}=0.38, (b) two heaters at their optimum positions, Y_{opt} = 0.09 and 0.49, (c) three heaters at their optimum positions, Y_{opt} = 0.06, 0.28 and 0.58.

In this case, the positions Y_{opt} are 0.05, 0.29 and 0.59 for the first, second and third heaters respectively, which correspond to the distance from the bottom to the first heater of 0.05 for the first heater, it is 0.14 between the first and second, and 0.20 between the second and third heaters. This clearly shows the optimum positioning of the three heaters with unequal distance between them. ψ_{ext} and θ_{max} are in this case -15.9682 (X=1, Y=0.6875) and 0.0873 respectively. As expected, the circulation is stronger with the three heater case with respect to the two heater case; otherwise, the appearance of the flow field is almost the same. The ambient air entrance section is further increased to 68.75% of the opening. The isotherms at the right hand side of Fig. 3.9(c) are with higher temperature gradients with respect to the case with two heaters; otherwise, they are similar.

3.4. Conclusion

We studied natural convection heat transfer in a square open cavity with discrete heat sources installed at the vertical wall facing the opening. The number of discrete heaters was from one to three; their size was varied from 0.05 to 0.20, and the Rayleigh number from 10^3 to 10^7. Conservation equations of mass, momentum and energy were solved by finite difference – control volume numerical method. At the beginning, the optimum positions of discrete heat sources were searched. Then, the heat transfer and volume flow rate were determined. In view of the results presented, the main points can be summarized as follows.

For best thermal performance of discrete heaters installed on the vertical wall facing the opening of a square cavity, the optimum positioning is not uniform with equidistance between them. The optimum positioning is obtained by maximizing the global performance. The heaters are positioned closer to each other at the beginning of the fluid flow. The final configuration of discrete heaters depends on Rayleigh number.

The maximum global conductance is quasi-independent of Rayleigh number for single and double heaters and h/L=0.05 at $Ra < 10^4$. The maximum global conductance is strongly Rayleigh number dependent in other cases; it increases with increasing Rayleigh number. Similarly, the maximum global conductance is increased with the number of heaters as well as with the heater size.

In determining the maximum conductance, we observe broad optima in C versus Y plots; in practical terms, this does not cause any difficulty in determining C_{max}. On the other hand, it shows that there is certain flexibility for positioning of the heaters if the technical circumstances require it.

At low Rayleigh numbers, $Ra < 10^4$, it is conduction dominated regime. At higher Rayleigh numbers, the convection becomes dominant regime. Generally, the Nusselt number and the volume flow rate are increasing function of the Rayleigh number, the heater size and the number of discrete heaters.

CHAPTER 4

CONJUGATE HEAT TRANSFER IN OPEN CAVITIES WITH A DISCRETE HEATER AT ITS OPTIMIZED POSITION

4.1. Introduction

The problem description, mathematical model and boundary conditions for this study have been presented in Chapter 2. This study and the results are submitted for publication [17]. We present in section 4.2, the optimization study results, in section 4.3, the parametric study results obtained with the discrete heating elements at their optimum position, and finally, in section 4.4, the main conclusions of this study. The variable geometrical parameters considered are, the aspect ratio, A = 0.5, 1 and 2, and the dimensionless wall thickness, ℓ/L = 0.05, 0.10 and 0.15. The dimensionless height of heating element was set as h/L = 0.15, 0.3 and 0.6 corresponding to A = 0.5, 1 and 2 respectively, which results in a constant ratio of the heater to cavity height. The Rayleigh number was varied from $Ra = 10^6$ to 10^{12}. The Prandtl number, Pr = 0.70 for air was kept constant. The conductivity ratio was varied from k_r =1 to 50. We note that due to conduction through to wall, part of the heat flux q'' is transferred through it, as a result of which the convection in the cavity is reduced, hence the Rayleigh number becames smaller. Thus, the range of the Rayleigh number is increased with respect to that of the case without conductive wall.

4.2. Optimization Study

We carried out studies to obtain the optimum position of the heating element by varying its position. The procedure was as follows: (i) We compute conductance $C(Y)$ at a constant Ra, (ii) we determine the maximum conduction, C_{max} at its optimum position Y_{opt}. We note that Y_{opt} in this study shows the lower edge position of the heater, yet C_{max} may be somewhat near the center of the heater. (iii) We repeat the steps (i) and (ii) to determine $C(Y)$, C_{max} and Y_{opt} at all the other Rayleigh numbers, from 10^6 to 10^{12}.

Typical results to obtain the conductance $C(Y)$ for the case of ℓ/L=0.10, h/L=0.30, A=1 and k_r=10 at Ra =10^6, 10^8 and 10^{10} are presented in Fig. 4.1(a). We can make the following observations: (i) for all the Rayleigh numbers, the conductance changes with the position of the heater. We have smaller conductance at the lowest position when the heater is at the bottom; the conductance is increasing rapidly as its position is raised reaching a broad maximum around $0.15<Y<0.55$ and it is decreasing thereafter to another low conductance at the top position. For example, at Ra=10^6, the maximum is when the lower edge of the heater is Y_{opt} = 0.30, which corresponds to the position of heater Y from 0.30 to 0.60. The center of the heater is at Y=0.45 for this case. This result is expected since the heat transfer regime at Ra = 10^6 is conduction dominated and the heater's optimum position is slightly off center at a lower position of the cavity, (ii) as the Rayleigh number is increased, the air flow as well as the conductance is increased. As we will see later, the heat transfer becomes by convection as well as conduction at Ra

$= 10^8$, the heater position is again at the same level, at $Y_{opt} = 0.30$. For $Ra = 10^{10}$, it is at $Y_{opt} = 0.40$. Following the increased air flow rate, the conductance, $C(Y)$ is increased accordingly, (iii) for all cases, we see broad maxima; we note that using the computation results or changing scale of conductance, it is not difficult to identify C_{max} at its Y_{opt}.

The effect of the conductivity ratio, k_r at $Ra=10^8$ is presented in Fig. 4.1(b) for the same case in Fig. 4.1(a). We see that the conductance is strongly affected by the conductivity ratio. Higher is the conductivity ratio, higher becomes the conductance. As the conductivity ratio is increased, ψ_{ext}/θ_{max} are both reduced since the heat transfer in the cavity is reduced for a given Rayleigh number. For example at $Ra = 10^8$, for $k_r = 1$, ψ_{ext}/θ_{max} = -12.8222/484.22E-6, for $k_r = 10$, ψ_{ext}/θ_{max} = -5.55695/82.82E-6 and for $k_r = 50$, ψ_{ext}/θ_{max} = -1.98097/17.32E-6. We see that both ψ_{ext}/θ_{max} are decreasing function of k_r. The optimum positions are $Y = 0.2$ for $k_r = 1$, 0.3 for $k_r = 10$ and 50.

To see the reason for the observations made with Fig. 4.1, we present streamlines and isotherms in Fig. 4.2 for the cases corresponding to Fig. 4.1 at $Ra=10^6$, 10^8 and 10^{10} (shown with (a), (b) and (c) respectively) and $k_r=1$ (the upper figure) and 10 (the lower figure) for each Rayleigh number. The heater size is $h/L=0.30$ and it is at its optimum position for each Rayleigh and conductivity ratio. We observe in Fig. 4.2(a) at $Ra=10^6$ that the heat transfer is convective for $k_r = 1$; it is conduction dominated for $k_r = 10$. This is expected since for $k_r = 1$, the wall having the same conductivity as that of the air, is insulated.

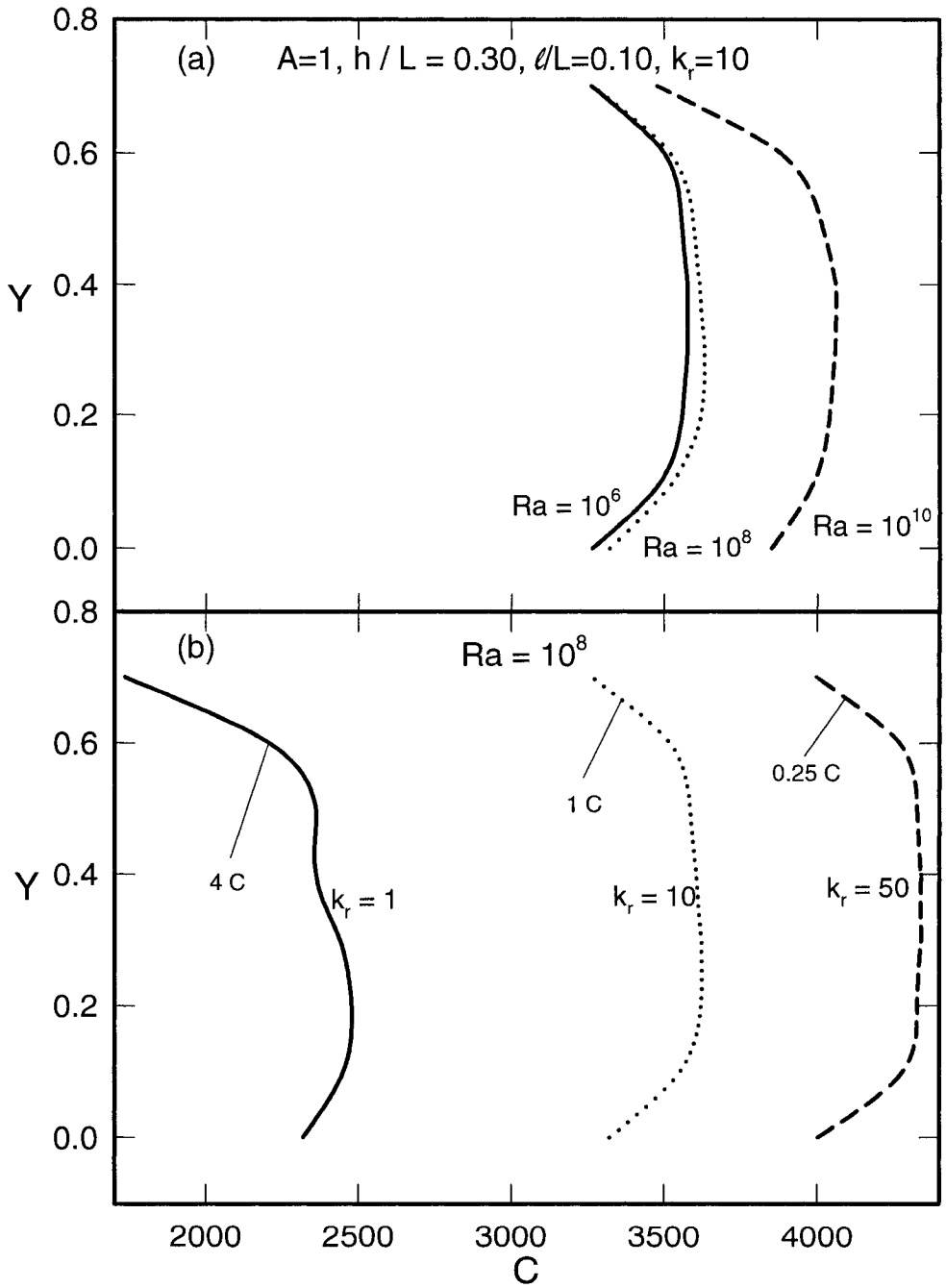

Figure 4.1: The maximization of the global conductance with the heat source of *h/L* =0.30. The scales of the curves for k_r=1 and 50 are 4C and 0.25C = abscissa value respectively.

Thus, the heat dissipated by the heater is mostly transferred by convection in the cavity. For k_r =10, a part of the heat goes through the wall and dissipated at the left side at θ= 0 and the rest is transferred by convection through the cavity opening.

Indeed, for k_r = 1, ψ_{ext}/θ_{max} = -1.0091893/632.9E-6, and for k_r = 10, -0.1262171/83.9E-6, which show highly increased convection and reduced maximum temperature for k_r = 1. At Ra = 10^8 in Fig. 4.2(b), for k_r = 1, ψ_{ext}/θ_{max} = -12.8222/484.22E-6, and for k_r = 10, -5.55695/82.82E-6. We see in this case a similar phenomenon to that at Ra = 10^6, however the convection becomes strong also with k_r = 10. Finally, at Ra=10^{10} in Fig. 4.2(c), for k_r = 1, ψ_{ext}/θ_{max} = -39.141833/290.03E-6, and for k_r = 10, -27.326857/74.07E-6, thus, the heat transfer is mainly by convection for both. Following our observations with Fig. 4.1(a), we see for k_r = 0.10 at the three Rayleigh numbers of Fig. 4.2 that there is no change in the circulation of air in the cavity at Ra = 10^6 and 10^8, hence the heater position is the same. At Ra = 10^{10}, the air circulation shifts upward and the heater position becomes higher. At Ra = 10^8 and for k_r = 1 and 10 of Fig. 4.1(b), again we see in Fig. 4.2(b) that the air circulation is relatively strong and sweeps lower level of the wall for k_r = 1. The heater position is at Y_{opt} = 0.20. In contrast, the air circulation is weaker and at higher level for k_r = 10, hence the heater position is at Y_{opt} = 0.30. Figs. 4.1 and 4.2 shows that the other parameters being constant, the optimum heater position is a strong function of the Rayleigh number as well as the conductivity ratio.

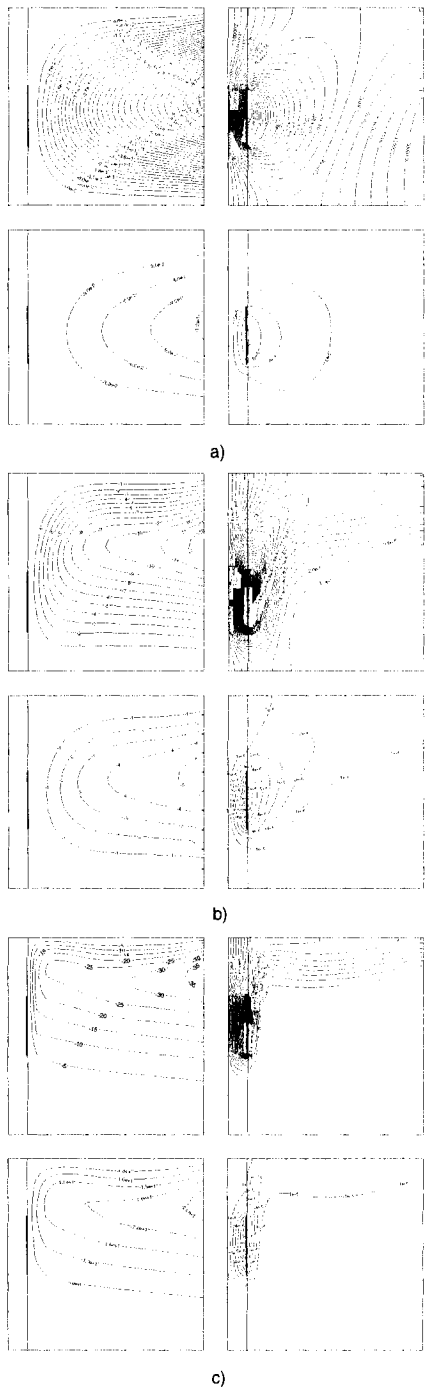

Figure 4.2: Streamlines (on the left) and isotherms (on the right) for A=1, ℓ/L =0.10, for a) Ra=10^6, b) Ra=10^8 and c) Ra=10^{10}. The upper figure is for k_r = 1 and the lower figure is for k_r = 10 for each case.

It was seen for the majority of the cases studied (not shown here) that the optimum heater positions Y_{opt} determined from the computed data were generally slightly decreasing function of the Rayleigh number, although in some cases, as observed in Fig. 4.2 for example, it was slightly increasing function. On the other hand, in most of the cases, Y_{opt} is found to be an increasing function of the conductivity ratio as observed earlier with Fig. 4.1. The maximum conductance, C_{max} obtained from the computed data showed for all cases that C_{max} is an increasing function of both Ra and k_r. For example, we present in Fig. 4.3, C_{max} as a function of Ra with k_r as a parameter for the case of A = 1, h/L=0.30 and k_r =1, 10 and 50. We see that C_{max} is an increasing function of both Ra and k_r. This dependence is stronger when the conductivity ratio is small. This is because, as we discussed earlier, k_r =1 corresponds to insulated wall case, in which the cooling is mainly by convection. As a result, θ_{max} is higher and by Eq. 9, C_{max} lower. For higher k_r, the cooling is by conduction through the wall and by convection in the cavity, hence the cooling is better, θ_{max} is smaller and C_{max} is higher.

4.3. Heat Transfer and Volume Flow Rate

The average normalized Nusselt number by Eq. (6) and the volume flow rate $\dot{V}$ by Eq. (7) are calculated as a function of Rayleigh number and presented in Fig. 4.4 for the case of A=1 with ℓ/L and k_r as parameters.

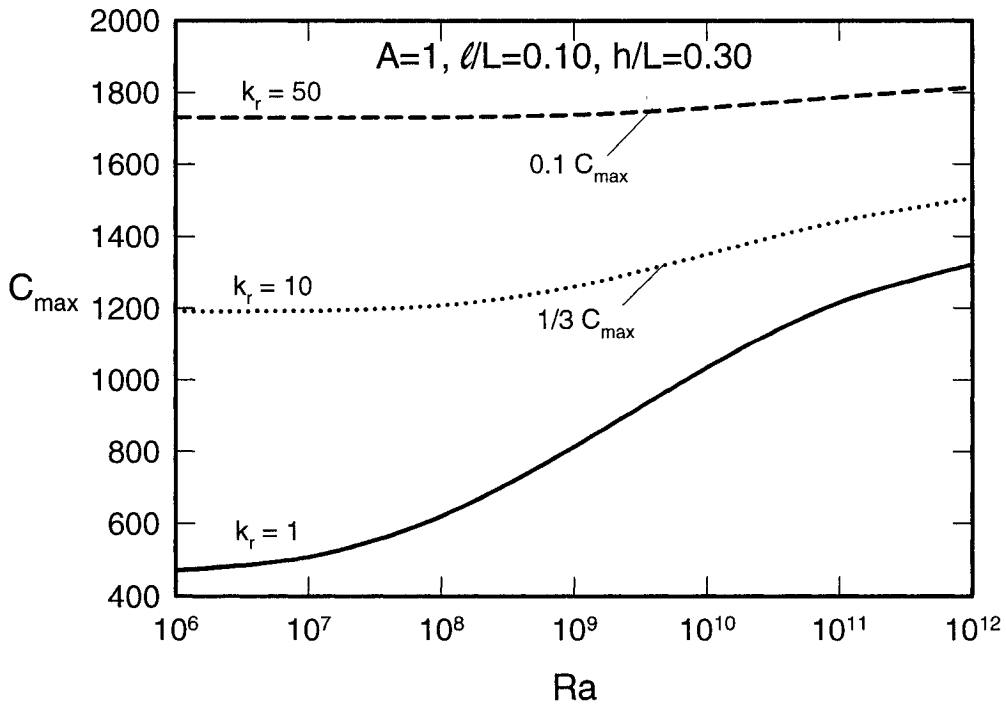

Figure 4.3: Maximum conductance as a function of the Rayleigh number with the conductivity ratio as a parameter. The scales of the curves for k_r=10 and 50 are $(1/3)C_{max}$ and $0.1C_{max}$ = ordinate value respectively.

For k_r=1, we see in Fig. 4.4(a) that *Nu* is an increasing function of *Ra* and ℓ/L. Starting at $Ra=10^6$, the heat transfer is by convection dominated. The Nusselt number is a weak function of the wall thickness since for k_r = 1, the wall is insulated and ℓ/L has a minor effect on the wall conductance. Nevertheless, we see that for ℓ/L=0.05 with respect to ℓ/L = 0.10 and 0.15, the conductance through the wall is relatively higher, i.e. the heat transfer by conduction is higher as a consequence of which convection is lower in the cavity at *Ra* from 10^6 to 10^8. Indeed, as the wall thickness is increased the conductance becomes smaller, the heat transfer by conduction through the wall is lower, and the

convection heat transfer in the cavity becomes dominant. At $Ra > 10^8$ the effect of ℓ/L on Nu is less. For k_r = 10, Fig. 4.4(b) shows a similar result, i.e. for ℓ/L=0.05 and 10 the convection starts at $Ra > 10^7$ above which it becomes dominant. The effect of ℓ/L on Nu is considerable: at $Ra > 10^7$, for ℓ/L =0.05, the wall conductance is relatively high, as a result of which Nu is relatively lower with respect to ℓ/L = 0.10 and 0.15.

For k_r = 50 in Fig. 4.4(c), the heat transfer is conduction dominated up to $Ra = 10^8$ above which the convection is the main heat transfer mode and the wall thickness ℓ/L has a relatively smaller effect on Nu. This is for the same reason as discussed above with Fig. 4.4(a). Thus, the heat transfer by conduction through the wall is increasing with increasing k_r as a consequence of which the heat transfer by convection in the cavity is relatively weaker. Generally, Nu is an increasing function of Ra, except at conduction dominated regime as observed in Fig. 4.4 (a)-(c).

The volume flow rate as a function Rayleigh number with k_r and ℓ/L as parameters is presented in Fig. 4.4 (d)-(f). Following the results in Fig. 4.4 (a)-(c), we observe that $\dot{V}$ is an increasing function of Ra and ℓ/L and decreasing function of k_r. At low Ra, since $\dot{V}$ is smaller, the difference for various ℓ/L is more discernable. Further, $\dot{V}$ is smaller for increasing k_r and decreasing ℓ/L. The same is true at higher Ra however due to logarithmic scale, they are less discernible.

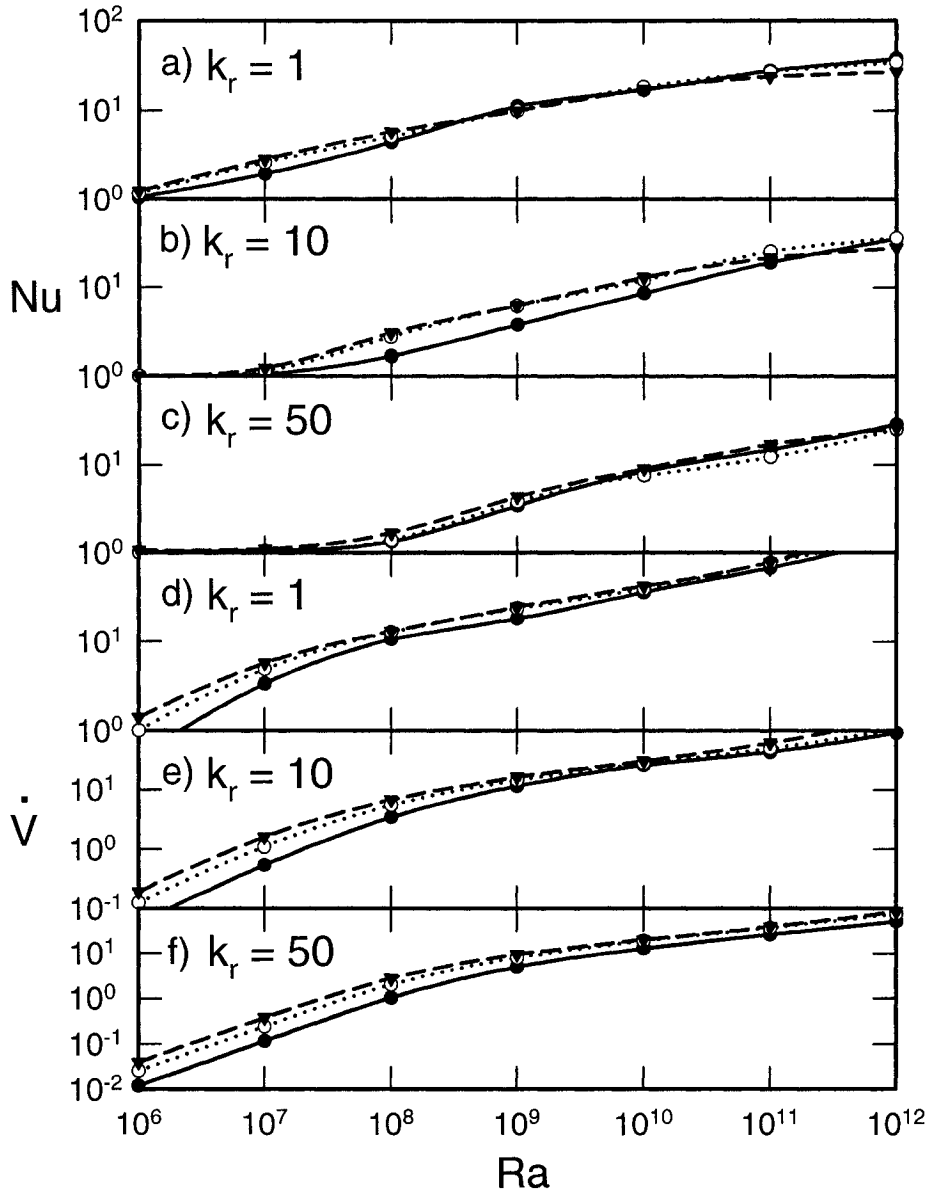

Figure 4.4: (a-c) Nusselt number and (d-f) volume flow rate as a function of Rayleigh number for A = 1 with ℓ/L and k_r as parameters. Solid line: ℓ/L =0.05, dotted line: ℓ/L =0.10, dashed line: ℓ/L =0.15.

We present Nu and $\dot{V}$ as a function of Ra with the cavity aspect ratio, A and ℓ/L as parameters in Fig. 4.5 (a)-(f). The other parameters are $k_r = 50$ and $h/L = 0.15$ for A = 0.05, $h/L = 0.30$ for $A = 1$ and $h/L = 0.60$ for $A = 0.60$. For $A = 0.5$, i.e. the shallow cavity, the heat transfer regime is by conduction at Ra from 10^6 to 10^8, even beyond for $\ell/L = 0.05$, thereafter it is convection dominated. Nu is an increasing function of Ra and ℓ/L.

As the cavity aspect ratio, A increases, the convection starts to be dominant regime at lower Ra numbers: for $A = 1$, i.e. square cavity, the convection starts at $Ra > 10^7$, and for $A = 2$, i.e. the tall cavity, it starts at $Ra > 10^6$. Nu is a weak function of ℓ/L for $A = 1$, and it is a strong function of it for $A = 2$. We see that for all cases of the cavity aspect ratio, Nu and $\dot{V}$ are an increasing function of Ra and ℓ/L.

The flow rate, $\dot{V}$ as a function of Ra with ℓ/L as a parameter is shown in Fig. 4.5 (d)-(f). We see that $\dot{V}$ is an increasing function of both Ra and ℓ/L for $A = 0.5$, 1 and 2. These results are expected following our observations in Fig. 4.5 (a-c). Generally, the flow rate is reduced with decreasing cavity aspect ratio, A.

Next, we will present the effects of the aspect ratio, A, the conductivity ratio, k_r and the wall thickness, ℓ/L on the Nusselt number and the volume flow rate.

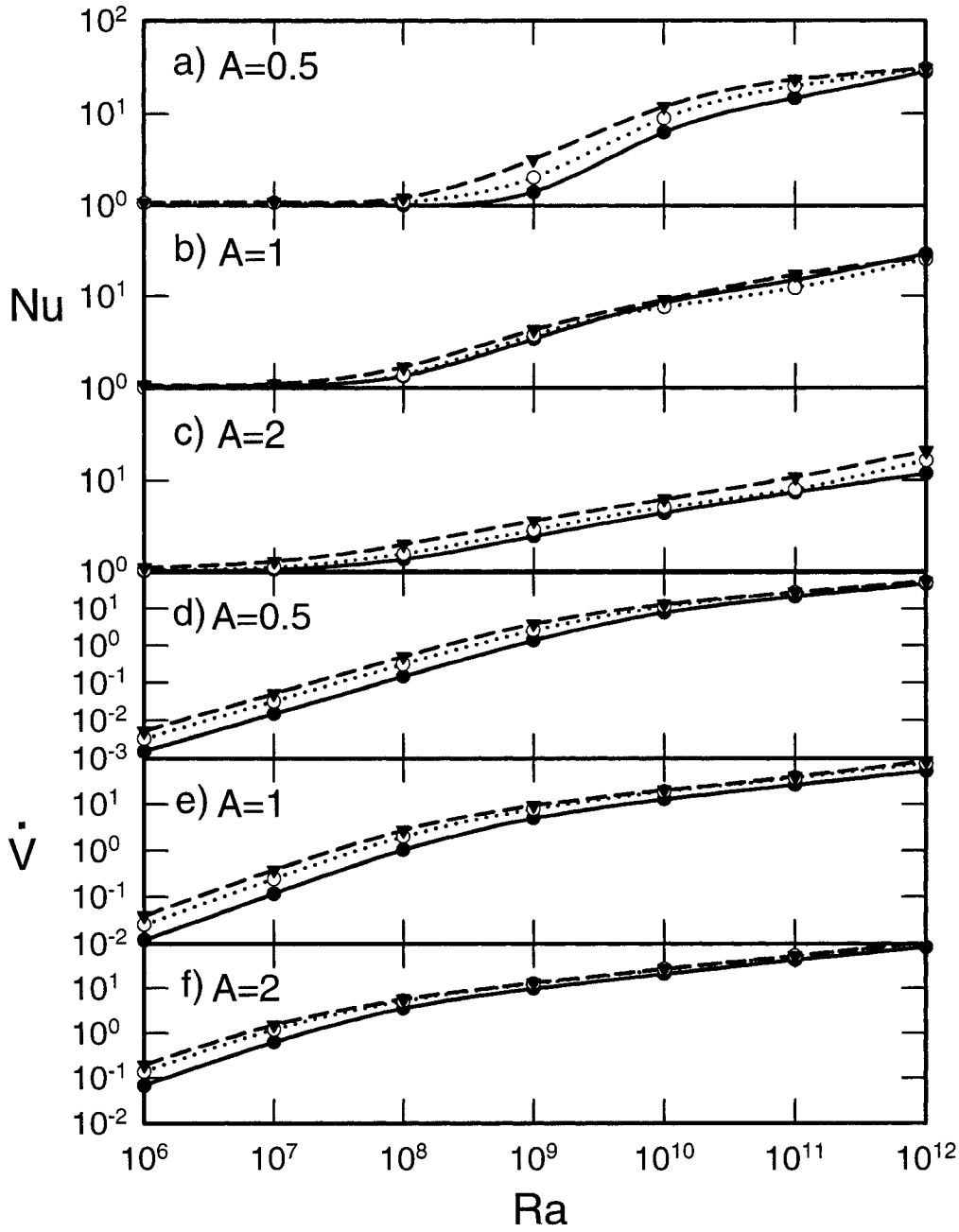

Figure 4.5: (a-c) Nusselt number and (d-f) volume flow rate as a function of Rayleigh number for k_r =50, h/L=0.15 for A=0.5, h/L=0.30 for A=1 and h/L=0.60 for A=2 with ℓ/L and A as parameters. Solid line: ℓ/L =0.05, dotted line: ℓ/L =0.10, dashed line: ℓ/L =0.15.

Figure 4.6 shows Nu and $\dot{V}$ as a function of A with Ra as a parameter while keeping ℓ/L=0.10 and k_r=50 constant. The heater length, h/L is variable with different aspect ratio, A, which is shown in the figure. It is noted that k_r=50 corresponds to the case with high conductance through the wall, as a result, relatively less convection in the cavity. We see in Fig. 4.6(a) that at low Rayleigh number, Ra=10^6, the heat transfer is conduction dominated, and $Nu \cong 1$ and almost the same for shallow, square and tall cavities.

At Ra=10^8 and A=0.5, i.e. a shallow cavity, the heat transfer is still conduction dominated; however, for square and tall cavities, convection is significant. The reason for the increased convection heat transfer at higher aspect ratios is due to increased flow through the relatively larger opening. Indeed, ψ_{ext} = -0.316515 for A = 0.5 and ψ_{ext} = -5.16181 for A = 2, thus showing the circulation is increased by 16 times. In contrast, Nu is increased by less than 1.5 times. At Ra=10^{10}, the heat transfer is convection dominated in all cases; Nu became a decreasing function of the aspect ratio. ψ_{ext} = -11.4165 and -26.2306 for A = 0.5 and 2 respectively, i.e. the circulation is increased by 2.3 times. Thus, the cooling is done by circulating more air through the cavity, as we will see next with Fig. 4.7, the maximum temperature is decreased, as a result of which Nu is decreased by 1.8 times. At still higher Rayleigh number, Ra = 10^{12} (not shown in Fig. 4.6), the Nusselt number was similarly a decreasing function of A. Fig. 4.6(b) shows $\dot{V}$ as a function of A for the same case; $\dot{V}$ is increasing with A from 0.5 to 2 at all Rayleigh numbers.

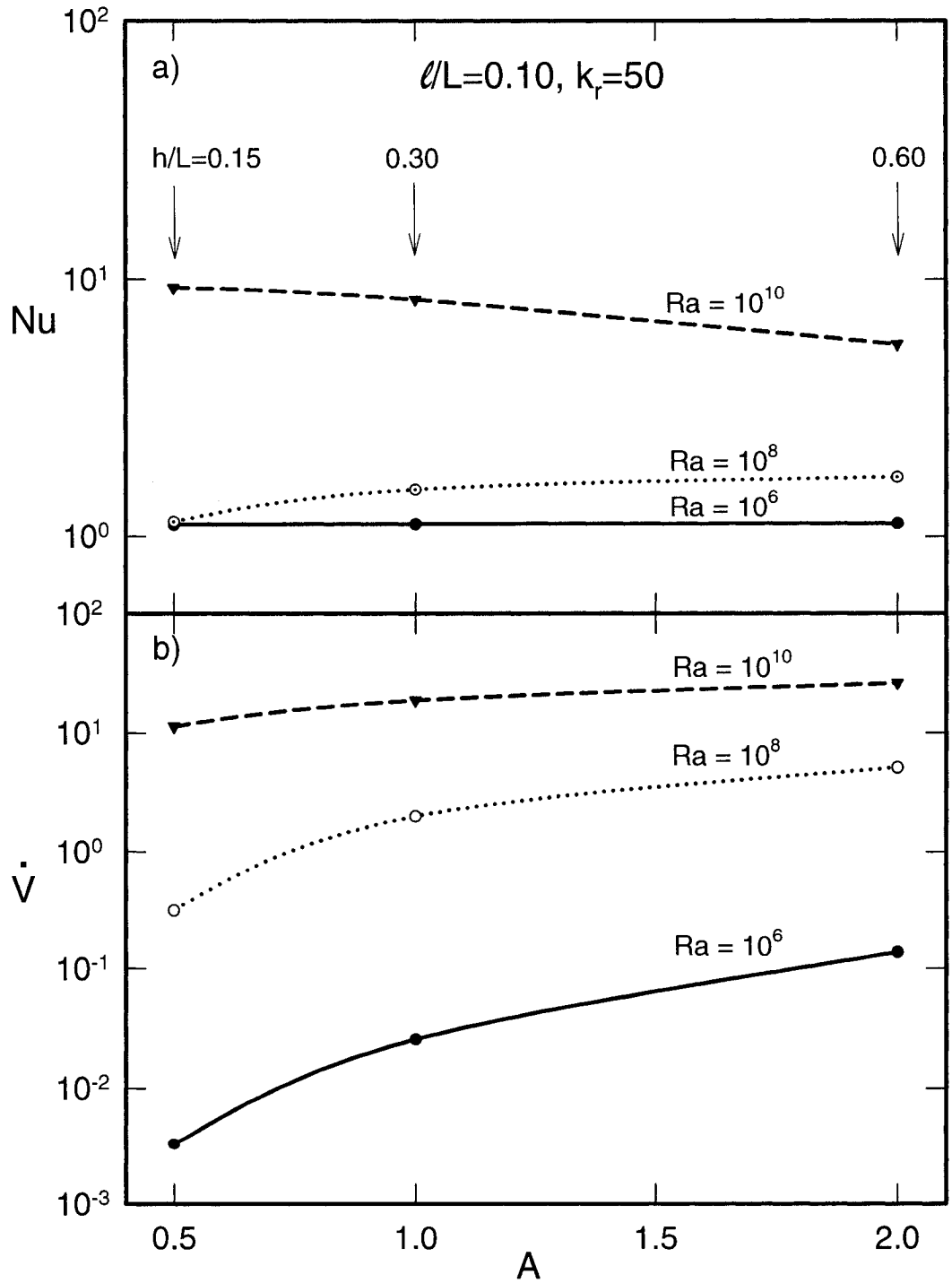

Figure 4.6: (a) Nusselt number and (b) volume flow rate as a function of the aspect ratio at various Rayleigh numbers.

At $Ra = 10^{10}$ for example, $\dot{V}$ is increased by 1.64 times when the aspect ratio, A changed from 0.5 to 1 and 1.4 times when it is changed from 1 to 2. The results show that the volume flow rate increases due to more efficient circulation through larger openings, like tall cavity. The flow rate $\dot{V}$ is a strong function of A at low Ra; it is less so as Ra increases. In fact, $\dot{V}$ for A from 0.5 to 2 increases about 42 times at $Ra = 10^6$ and about 1.8 times at $Ra = 10^{12}$.

To see the reason for changes in the volume flow rate and heat transfer with cavity aspect ratio, the streamlines and isotherms for the same case of Fig. 4.6 at $Ra=10^8$ are traced and presented in Fig. 4.7 for $A = 0.5$, 1 and 2. ψ_{ext}/θ_{max} for A=0.5, 1 and 2 in Fig. 4.7 (a), (b) and (c) are -0.316515/27.76E-6, -2.01127/17.33E-6 and -5.16181/9.36E-6 respectively. The streamlines and isotherms show that the flow in the shallow cavity is weak and the maximum temperature is high; in contrast, in the square cavity, the circulation intensity is increased by 15% and the maximum temperature is reduced by 36%. For the tall cavity, the circulation intensity is increased further by 157% and the maximum temperature is decreased by 50%. We see that the aspect ratio is a strong parameter affecting the maximum temperature and as a result the heat transfer as observed with Fig. 4.6.

The effect of k_r on Nu and $\dot{V}$ for the case of A=1, h/L=0.30 and ℓ/L=0.10 is presented in Fig. 4.8 at $Ra=10^6$, 10^8 and 10^{10}. We see that both Nu and $\dot{V}$ are decreasing function of k_r at all three Rayleigh numbers.

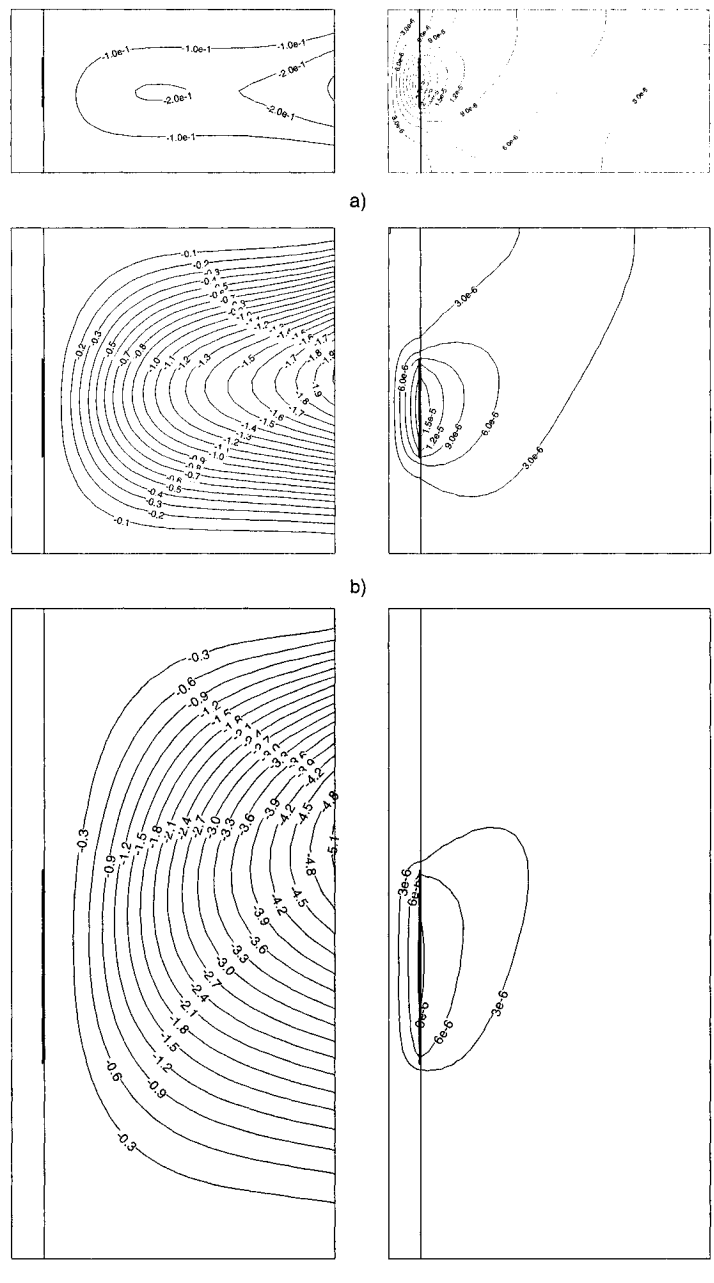

Figure 4.7: Streamlines (on the left) and isotherms (on the right) for the case of Fig. 4.6 (ℓ/L =0.10, k_r = 50) and Ra=10^8. a) A=0.5, h/L = 0.15, b) A=1, h/L = 0.30, and c) A=2, h/L = 0.60.

At $Ra=10^6$, the heat transfer is conduction dominated and it is less dependent on k_r. At higher Rayleigh numbers, following earlier observations with Figs. 4.4 and 4.5, the results are: as k_r is increased, the conductance is increased, as a result of which the heat transfer and the volume flow rate in the cavity are decreased. We see that k_r is a strong parameter affecting the heat transfer and flow rate in the cavity.

The effect of the wall thickness, ℓ/L on Nu and $\dot{V}$ for the same case of Fig. 4.8 but with $k_r=50$ is presented in Fig. 4.9 at the same three Rayleigh numbers. Generally, Nu and $\dot{V}$ are an increasing function of ℓ/L, except for Nu at $Ra=10^6$. As the wall thickness is increased, the conductance through the wall is decreased; as a result, the heat transfer and the volume flow rate are increased through the open cavity. However, we see that the effect of the wall thickness at high Rayleigh numbers is not too significant.

4.4. Conclusion

We studied natural convection heat transfer in open cavities with a discrete heat source installed at its optimum position at the vertical wall with finite thickness facing the opening. The aspect ratio was varied from 0.5 to 2, the wall thickness from 0.05 to 0.15 and the heater size from 0.15 to 0.60. The Rayleigh number varied from 10^6 to 10^{12}, the conductivity ratio from 1 to 50; the Prandtl number was 0.7.

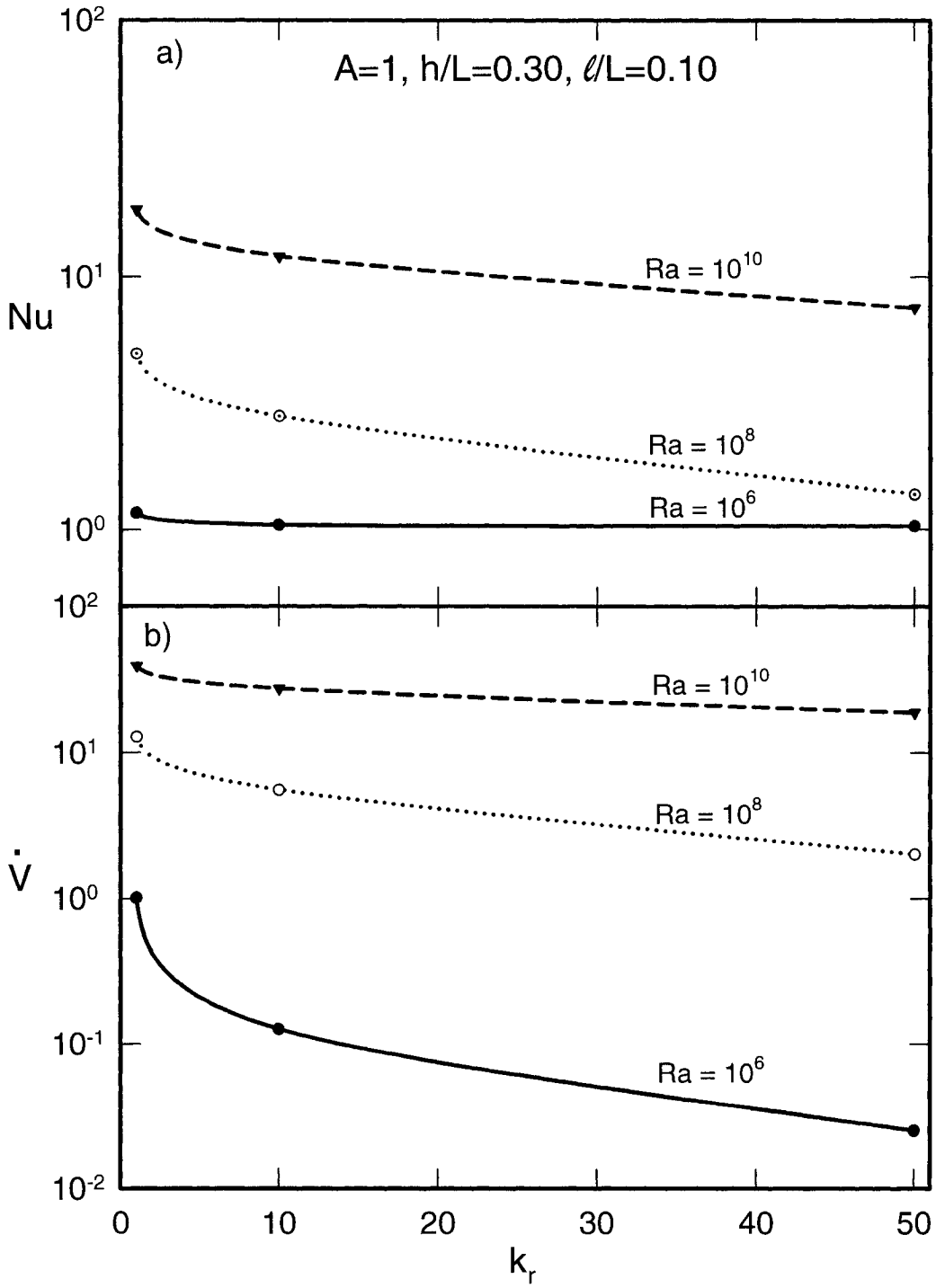

Figure 4.8: (a) Nusselt number and (b) flow rate as a function of the conductivity ratio with the Rayleigh number as a parameter.

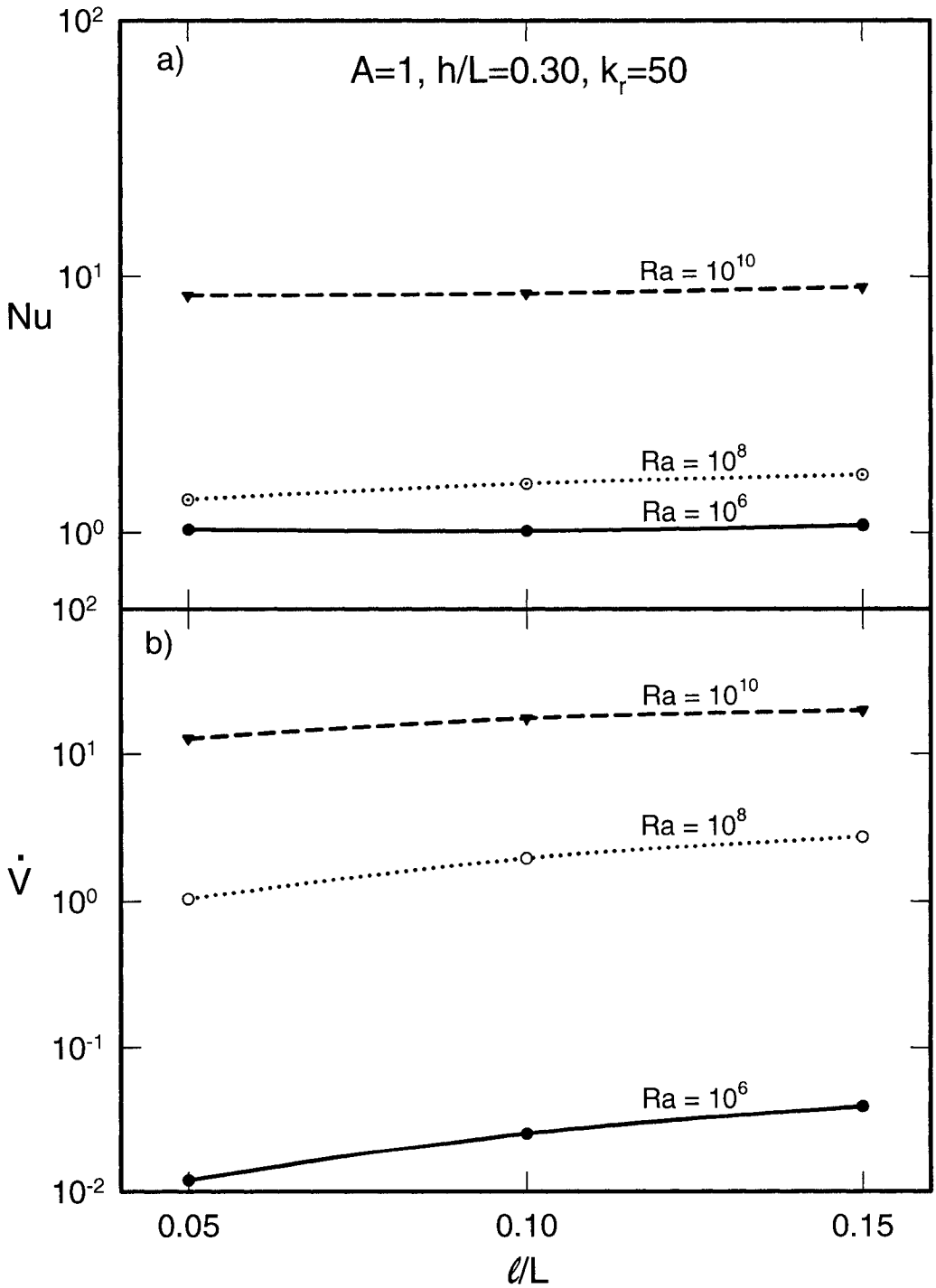

Figure 4.9: (a) Nusselt number and (b) volume flow rate as a function of the wall thickness with the Rayleigh number as a parameter.

Conservation equations of mass, momentum and energy were solved by finite difference–control volume numerical method. At the beginning, the optimum position of discrete heat source was determined. Then, the heat transfer and volume flow rate were determined. In view of the results presented, the main points can be summarized as follows.

The optimum position of a discrete heater in an open cavity is usually at its off center. Its position depends on the Rayleigh number, the conductivity ratio of the wall, the aspect ratio of the cavity and the wall thickness.

In determining the maximum conductance, we observed broad optima. However, this did not cause any difficulty in determining the position of heaters since numerical results clearly showed the maximum conductance and its coordinates. On the other hand, we note broad optima may give certain flexibility for positioning of the heater if the circumstances require it.

Depending on the cavity aspect ratio and the conductivity ratio, the heat transfer is conduction dominated at low Rayleigh numbers, Ra from 10^6 to 10^8; it is convection dominated regime at higher Rayleigh numbers up to 10^{12} in this study. Generally, the Nusselt number and the volume flow rate are increasing functions of the Rayleigh number and the wall thickness. The Rayleigh number is a decreasing function of the cavity aspect ratio and the conductivity ratio. The volume flow rate is an increasing

function of the cavity aspect ratio and a decreasing function of the conductivity ratio. *Ra, A,* k_r are significant and ℓ/L is relatively less significant parameters affecting thermal performance of discrete heaters at their optimum positions.

CHAPTER 5

GENERAL CONCLUSION

5.1. Introduction

We studied natural convection and conjugate heat transfer in open cavities with discrete heat sources installed at the vertical surface facing the opening. We considered the cases with or without a massive wall, on which heaters are installed. The number of discrete heaters may be variable; depending on the case studied, their size was varied from 0.05 to 0.30, and the Rayleigh number from 10^3 to 10^{12}. Conservation equations of mass, momentum and energy were solved by finite difference – control volume numerical method. At the beginning, the optimum positions of discrete heat sources were searched. Then, the heat transfer and volume flow rate were determined. In view of the results presented, the main points can be summarized as follows.

5.2. In Case of Open Cavity without a Massive Wall and Single or Multi-Heaters

- For best thermal performance of discrete heaters installed on the vertical wall facing the opening of a square cavity, the optimum positioning is not uniform with equidistance between them. The optimum positioning is obtained by maximizing the global performance. The heaters are positioned closer to each

other at the beginning of the fluid flow. The final configuration of discrete heaters depends on Rayleigh number.

- The maximum global conductance is quasi-independent of Rayleigh number for single and double heaters and h/L=0.05 at $Ra < 10^4$. The maximum global conductance is strongly Rayleigh number dependent in other cases; it increases with increasing Rayleigh number. Similarly, the maximum global conductance is increased with the number of heaters as well as with the heater size.

- At low Rayleigh numbers, $Ra < 10^4$, the convection is conduction dominated a higher Rayleigh numbers, it becomes convection dominated regime. Generally, the Nusselt number and the volume flow rate are increasing functions of the Rayleigh number, the heater size and the number of discrete heaters.

5.3. In Case of Open Cavity with a Massive Wall and Single-Heater

- The optimum position of a discrete heater in an open cavity is usually at its off center. Its position depends on the Rayleigh number, the conductivity ratio of the wall, the aspect ratio of the cavity and the wall thickness.

- Depending on the cavity aspect ratio and the conductivity ratio, the heat transfer is conduction dominated at low Rayleigh numbers, Ra from 10^6 to 10^8; it is

convection dominated at higher Rayleigh numbers up to 10^{12} in this study. Generally, the Nusselt number and the volume flow rate are increasing functions of the Rayleigh number and the wall thickness. The Rayleigh number is a decreasing function of the cavity aspect ratio and the conductivity ratio, the volume flow rate is an increasing function of the cavity aspect ratio and a decreasing function of the conductivity ratio. *Ra, A,* k_r are significant and ℓ/L is relatively less significant parameters affecting thermal performance of discrete heaters at their optimum positions.

- In certain cases with or without conductive wall, in determining the maximum conductance, we observed broad optima in C versus Y plots. In practical terms, this did not cause any difficulty in determining the position of heaters since the numerical results clearly showed the maximum conductance and its coordinates. On the other hand, we note that broad optima may give certain flexibility for positioning of the heater if the circumstances require it.

REFERENCES

[1] H.Y. Wang, F. Penot, J.B. Sauliner, Numerical study of a buoyancy-induced flow along a vertical plate with discretely heated integrated circuit packages, Int. J. Heat Mass Transfer 40 (1997) 1509-1520.

[2] Y. liu, N. Phan-Thien, An optimum spacing problem for three chips mounted on a vertical substrate in an enclosure, Numer. Heat Transfer A 37 (2000) 613-630.

[3] A.K. da Silva, S. Lorente, A. Bejan, Optimal distribution of discrete heat sources on a wall with natural convection, Int. J. Heat Mass Transfer 47 (2004) 203-214.

[4] A.K. da Silva, S. Lorente, A. Bejan, Optimal distribution of discrete heat sources on a plate with laminar forced convection, Int. J. Heat Mass Transfer 47 (2004) 2139-2148.

[5] A.K. da Silva, S. Lorente, A. Bejan, Maximal heat transfer density in vertical morphing channels with natural convection, Numer. Heat Transfer A 45 (2004) 135-152.

[6] A.K. da Silva, G. Lorenzini, A. Bejan, Distribution of heat sources in vertical open channels with natural convection, Int. J. Heat Mass Transfer 48 (2005) 1462-1469.

[7] A.K. da Silva, L. Gosselin, Optimal geometry of L and C-shaped channels for maximum heat transfer in natural convection, Int. J. Heat Mass Transfer 48 (2005) 609-620.

[8] P. Le Quere, J.A.C. Humphrey, F.S. Sherman, Numerical calculation of thermally driven two-dimensional unsteady laminar flow in cavities of rectangular cross section, Numer. Heat Transfer 4 (1981) 249–283.

[9] F. Penot, Numerical calculation of two-dimensional natural convection in isothermal open cavities, Numer. Heat Transfer 5 (1982) 421–437.

[10] Y.L. Chan, C.L. Tien, A numerical study of two-dimensional natural convection in square open cavities, Numer. Heat Transfer 8 (1985) 65–80.

[11] A.A. Mohamad, Natural convection in open cavities and slots, Numer. Heat Transfer 27 (1995) 705–716.

[12] O. Polat, E. Bilgen, Laminar natural convection in inclined open shallow cavities, Int. J. Therm. Sci. 41 (2002) 360–368.

[13] O. Polat, E. Bilgen, Conjugate heat transfer in inclined open shallow cavities, Int. J. Heat Mass Transfer 46 (2003) 1563-1573.

[14] S.V. Patankar, Numerical Heat Transfer and Fluid Flow, Hemisphere Publishing Corporation, New York, 1980.

[15] D. de Vahl Davis, Natural convection of air in a square cavity: a benchmark solution. Int. J. Num. Methods Fluids 3 (1983) 249-264.

[16] A. Muftuoglu, E. Bilgen, Natural convection in an open square cavity with discrete heaters at their optimized positions. Int. J. Thermal Sciences. In press, March 2007.

[17] A. Muftuoglu, E. Bilgen, Conjugate heat transfer in open cavities with a discrete heater at its optimized position. Int. J. Heat Mass Transfer. In press, April 2007.